



Anal. Bioanal. Chem. Res., Vol. 11, No. 4, 361-386, September 2024.

Synthesis Method of Stable Metal-Organic Framework (MOF) Based Nanomaterials and Their Multifaceted Application

Abdu Hussien Ali^{a,*}, Walelign Wubet Melkamu^a, Aklilu Melese Mengesha^b, Molla Tefera Negash^c and Kenaegzer Mulate^d

^aDepartment of Chemistry College of Natural and Computational Sciences, Mekdela Amba University, Ethiopia

^{a,c}Department of Chemistry, College of Natural and Computational Sciences, University of Gondar, Ethiopia

^{b,d}Department of Chemistry College of Natural and Computational Sciences, Kebridehar University, Ethiopia

(Received 8 January 2024, Accepted 27 April 2024)

Metal-organic frameworks (MOFs), formed by the self-assembly of metal centers or clusters and organic linkers, possess many key structural and chemical features. MOFs are generally synthesized by employing a modular synthesis, where crystals are slowly grown from a hot solution by nucleation and growth mechanism to form porous structures. The advantages and applications of many MOFs are ultimately limited by their stability under harsh conditions. The factors that affect MOF stability under certain chemical environments are introduced to guide the design of robust structures. Therefore, stable MOFs are formed by using different techniques including modulated synthesis (spray drying, electrochemical, microwave-assisted, mechanochemical synthesis, and microfluidic synthesis method). In particular, their high porosity, large surface area, tunable chemical composition, high degree of crystallinity, and potential for post-synthetic modification for molecular recognition make stable MOFs promising candidates for many implicated in the industry such as photocatalysis, hydrogen storage, adsorption, carbon capture, energy storage, biomedical application (drug delivery, antibacterial, biocatalysis, and biological imaging) and sensing (fluorescent and electrochemical). Overall, this review is expected to guide the design of stable MOFs by providing insights into existing structures, which could lead to the discovery and development of more advanced functional materials for different applications.

Keywords: MOF, Modification, Stability, Modular synthesis

INTRODUCTION

Nanomaterials relate to materials with at least one dimension at the nanometer size (1-100 nm), the corresponding aggregates or composed of them as introductory units in three-dimensional space, and have gained great attention since their emergence [1]. Especially, metal-organic frameworks (MOFs) based nanomaterials are organic-inorganic hybrid micro- or nano-crystalline porous coordination polymer materials. Therefore, nano-sized MOFs have uniform size and good mono-dispersity. Accordingly, well-defined nano-sized MOFs with precision

in size and morphology have been drawing attention in recent years. Yet, controlling the shape and size of MOFs is challenging, particularly for nano-sized MOFs. The metal salts, aromatic co-solvents, pH, temperature, reagent concentrations, and time for the synthesis of MOFs must be carefully selected as small variations in reaction conditions have significant effects on the quality of the product [2-4]. Generally, nano-sized MOF materials consist of a regular array of positively charged metal ions surrounded by organic 'linker' molecules to form one-, two-, or three-dimensional structures. The d-block transition rudiments with high coordination numbers such as Zn, Cu, Co, and Fe are chosen as metal ions, while multi-dentate organic ligands with a rigid backbone such as benzene-1,4-dicarboxylic acid (BDC),

*Corresponding author. E-mail: abdelmelik9@gmail.com

benzene-1,3,5-tricarboxylic acid (BTC), naphthalene-1,4-dicarboxylic acid and 2-ethyl-1*H*-imidazole are used as linkers. The metal ions form nodes that bind the arms of the linkers together to form a repeating, pen- suchlike structure. Due to this concave structure, it has an extraordinarily large internal surface area. MOFs based materials have ultra-low density, high surface area, and regular pore structure when compared with the traditional porous materials like active carbons or zeolites, MOFs demonstrate more flexibility in tuning the structure and surface chemistry [5]. It also offers unique structural diversity in contrast to other previous porous materials – uniform pore structures; atomic-level structural uniformity; tunable porosity; extensive varieties; and flexibility in network topology, geometry, dimension, and chemical functionality [6].

The discovery of MOFs was derived from the study of Prussian blue-Fe coordination polymers [7]. After a variety of coordination polymers, the final MOF-5 ($[Zn_4O(BDC)_3](DMF)_8(C_6H_5Cl)_2$) ($H_2BDC = 1,4$ -phthalic acid, DMF = *N,N*-dimethylformamide) was proposed. This MOF-5 broke the historic world record of porosity at that time by showing a very high surface area of $6,500 \text{ m}^2 \text{ g}^{-1}$. This discovery of MOF-5 is recognized as the most prominent example of a metal-organic framework by many researchers. They are different functional groups with different functional groups of organic skeleton compounds that continue to appear, such as ZIF, MIL, ZMOF, MPF, MAF, MBioF, mesoMOF, and so on. The metal-organic frameworks (MOFs) were named after the universities in which the materials were prepared and the researchers who synthesized the materials. The most common are UiO-66 (University of Oslo), MIL (Materials Institute Lavoisier), HKUST (Hong Kong University of Science and Technology), ITQMOF (Instituto de Tecnología Química metal-organic framework), SNU (Seoul National University), JUC (Jilin University China), CUK (Cambridge University KRICT), and POST (Pohang University of Science and Technology), *etc.*, are after the university names [8]. As the geometric composition of materials, size, and function can be flexible changes, more than 2000 MOF structures have been reported and studied only in the past ten years [9].

MOFs are conventionally synthesized by employing a modular synthesis, where crystals are slowly grown from a hot solution by nucleation and growth mechanism to form

porous structures [10]. The different linkers resulted in different pore sizes, surface areas, and different chemical properties. These properties gained lots of interest leading several researchers to use another synthetic method, to functionalize and modify these materials. Therefore, there are different synthesis methods to obtain metal-organic framework structures have been developed over the last three decades using a wide range of parameters such as temperatures, solvent compositions, type of solvent, reagent ratios, reagent concentrations, and reaction times [11]. Some of the common techniques used for the synthesis of MOFs are solvothermal synthesis [12], microwave heating [13], sonication-assisted synthesis [14], mechanochemical procedures [15], solid-state synthesis [16], spray drying [17] and electro-synthetic deposition [18].

MOFs-based nanomaterials have received considerable attention in the last decade rather than other nanomaterials [19] due to their possessing large surface areas, high porosity, tunable structural, and robust thermal stability [20,21]. They have arisen as interesting materials for various applications like gas separation and purification [22] (for selective H_2 adsorption [23], selective adsorption of CO_2 [24], and CH_4 [25], hydro-carbon separation [26], selective adsorption of O_2 [27]), targeted drug delivery [28,29], optical and luminescent materials [30-34], catalysts [35] (enantioselective chiral reactions [36] asymmetric epoxidation of alkenes [37] and allyl alcohols [38], opening of epoxides with methanol [39], benzaldehyde activation [40], oxidation of alcohols [41], allyl oxidation of cyclohexene [42], the Suzuki [24], and Sonogashira reactions [43],) photocatalysis, energy storage [44], sensor [45], magnetism [46], and others.

There are different review papers about MOF have been published. However, this review focuses on a detailed and clear description of the synthesis method, stability, mechanical properties, and diverse application of metal-organic frameworks-based nanomaterial. Major attention is paid to specific features caused by the unique structure of these porous compounds. In particular, synthetic methods and modifications used to prepare nano-sized MOFs of various dimensionality and porosity, and skeletons to their potential applications in the adsorption of many compounds, such as biologically important compounds (drugs, antibiotics, *etc.*), photocatalysis, toxic pollutants, and gas, electrochemical energy storage systems and sensors,

catalysts and electrocatalysts, and efficient drug delivery carriers which is essential for the understanding of the MOF activity and not clearly described yet before.

SYNTHESIS METHOD AND PROPERTIES OF STABLE MOF NANOMATERIAL

General Synthesis Method

The first method for the synthesis of MOFs is solvothermal. Classically, metal precursors and organic linkers are dissolved in the solvent and placed in a closed reaction vessel for the formation and self-assembly of MOF crystals. Now a day much research and development, have been done in the synthesis of MOFs. New synthesis methods such as spray drying, electrochemical, microwave-assisted, mechanochemical synthesis, microfluidic synthesis methods, etc. have all been reported as described in Fig. 1 below [47]. In most techniques, the development of the MOFs is performed in the liquid phase by mixing solutions of the ligand and the metal salt.

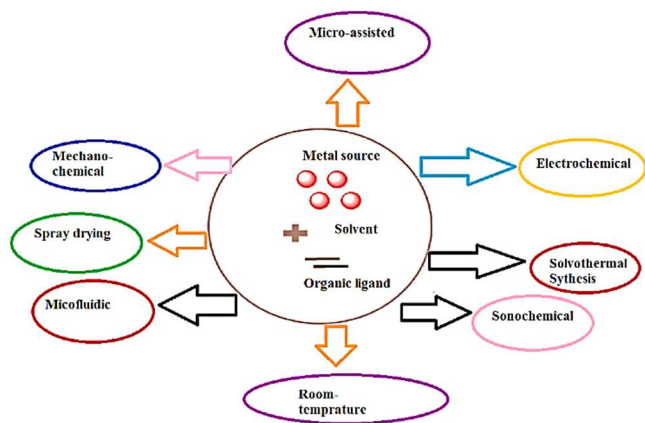


Fig. 1. The most common synthesis approaches of MOFs.

The main aim during synthesis is the ability to control and tailor the morphology and size and the chemical functionalization of MOF crystals is dynamic in delivering targeted properties and performances of the resulting MOF materials. The following provides an overview of the currently developed modulated synthesis methods for morphology and size control of MOF crystals and doping to create hybrid MOF crystals.

Solvothermal method. The term solvothermal refers to the operation of any detergent in the synthesis process [48]. This fashion includes a detergent (*e.g.*, dimethyl formamide, ethanol, methanol, acetone, and water) based reaction of metal salts with organic ligands and crystallization in a closed vessel (autoclave or sealed container), where high pressure and temperature (at or beyond a solvent’s boiling point) ease the self-assembly and crystal development (Fig. 2). The major advantage of a solvothermal system is the comparatively advanced yield of products. Still, the crystallinity, morphology, structure, size, and yield of synthesized MOFs are sensitively affected substantially by the cooling speed rate at the end of the response.



Fig. 2. Typical solvothermal synthesis method.

Generally, a solvothermal system is the most effective and universal strategy for preparing nanoMOFs therefore far. In the initial period, the foremost arguments similar to stoichiometric ratio, response time, pH, and temperature are concentrated to regulate the size of MOF crystals [49]. Also, some nanoMOFs (Fe-MIL-88A [50], Fe-MIL-89, MOF-5 [51], ZIF-8 [52], and ZIF-90 [53]) can be synthesized by directly regulating the above parameters. It is also used to synthesize different structures with zeolite-like morphology, incorporating zinc (ZIF-1, 4, 6, 8, 10, 11) or cobalt (ZIF-9,12) and imidazole derivation as linkers.

Electrochemical synthesis method. In MOF synthesis by an electrochemical system (Fig. 3), the metal ions are continuously introduced to the reaction medium through anodic dissolution for sufficient response with molecular ligands. Enhanced ion strength in the reaction medium *via* precluding electrostatic attractions can inhibit the metal ion deposition on the cathode [54]. The metal ions are supplied in the reaction mixture containing dissolved linker moles and

an electrolyte through the dissolution of the anode. This also makes it possible to avoid the formation of anions in the course of the reaction and to initiate a continuous process, which is essential for going to the product of fairly large quantities of MOFs. The advantage of electrochemical approaches is avoiding anions such as nitrates from metal salts, lower temperatures of reaction, and extremely quick synthesis.

An electrochemical system was first used for the synthesis of HKUST-1 MOF in 2005. These synthesis styles of MOFs gave homologous surface areas and pore sizes. A thin layer of HKUST-1 was electrically deposited on a copper mesh, which was used as the anode. Thus, this method allows to production of both powders and film forms of MOF [55,56].

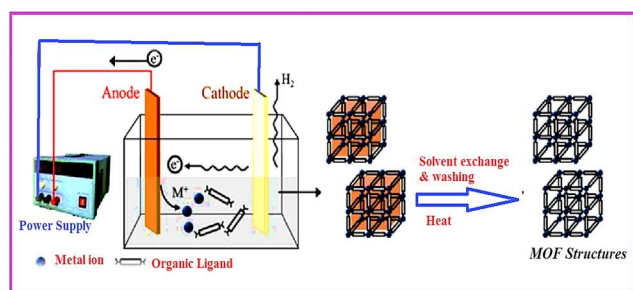


Fig. 3. Electrochemical synthesis method of MOF. Reprinted by permission from reference [54], Copyright © 2013, Korean Institute of Chemical Engineers.

Room Temperature synthesis method. Room temperature synthesis (RTS) of MOFs refers to the synthesis in ambient conditions without an external heating procedure. The RTS includes stepwise and direct methods. The former represents the strategies with multiple steps, including the pre-treatment of organic ligands or inorganic metal cations, and the pre-synthesis of inorganic sub-units (*e.g.*, Fe oxo trimer, Ti oxo clusters, Zr oxo clusters). Room-temperature syntheses are crucial for integrating functional compounds, especially in water-stable MOFs [57]. This type of method focuses on the direct preparation of MOFs under more sustainable conditions. MOFs are synthesized at room temperature, and thus the harmful organic solvents are replaced partly by water. As described in Fig. 4 below, this

method is based on the addition of a modified substrate group or other electron donor group to a joint metal and ligand solution and also allows the deprotonation of the ligand, leading it to react with the metal ion in the solution. Therefore, this resulted from the precipitation occurring by the abrupt change of pH.

Gu and his team proposed a salting-in species-induced self-assembly (SSISA) strategy based on the Hofmeister effect to synthesize a series of pure Ce-UiO-66-X (-H, -CH₃, -Br, -NO₂) can be synthesized at room temperature within 10 min to 6 h. Ce (IV)-MOFs are another class of tetravalent MOFs which having unique photo-redox properties, showing many structural similarities to the well-known Zr-MOFs [58]. In most cases of MOF synthesis, BDC was used as a model ligand due to its intensive use in MOF development. The salting anions like NO₃⁻, ClO₄⁻, SCN⁻, and I⁻ significantly enhance the solubility of BDC in an aqueous solution. This effect results in the decrease in activation energy of MOF nucleation to permit the MOF formation at room temperature. Yet, these RT Ce-UiO-66-X need to be well-washed with DMF after the synthesis, particularly when using pristine BDC, probably due to the incomplete crystallization of MOFs in these conditions. In recent years, most researchers using ionic liquids (ILs) as a solvent to produce high-quality UiO-66 at room temperature, and can also be simply controlled size from 30 nm to 80 nm by changing the anions and cations of ILs. Ionic liquids can act as both solvents and structure-directing agents, providing a medium for the formation and growth of MOF crystals. Their unique physicochemical properties, such as low vapor pressure and high polarity, can influence the nucleation and crystal growth process. Briefly, to control the size of UiO-66 using ILS, specific ionic liquid solvents can be selected based on their ability to interact with the metal ions and organic linkers involved in the MOF synthesis. By adjusting factors such as the concentration of the ionic liquid, reaction temperature, and reaction time, it is possible to manipulate the growth kinetics and obtain UiO-66 crystals with desired sizes.

Microwave-assisted method. Microwave-assisted techniques have been widely applied to the rapid synthesis of nanopore materials under solvothermal/hydrothermal conditions. The energy used for the reaction in this method is obtained in the form of microwave radiation described in Fig. 5 below. MOFs (Metal-Organic Frameworks)

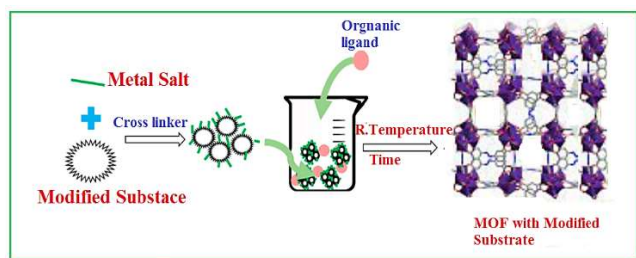


Fig. 4. General feature of room temperature synthesis method.

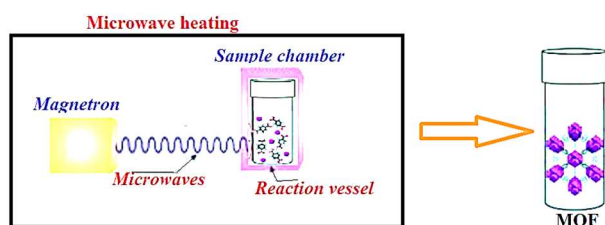


Fig. 5. Systematic representation of Microwave-assisted synthesis method of MOF.

synthesized by microwave possess some distinct characteristics. Here are some general characteristics of MOFs synthesized using these techniques: microwave methods offer accelerated synthesis compared to conventional methods. The application of microwave irradiation promotes faster reactions and shorter reaction times, resulting in reduced synthesis times for MOFs [59]. It also enhances crystallinity, in which the controlled and rapid energy input in these methods promotes efficient nucleation and crystal growth, resulting in well-defined and highly crystalline MOF structures. In addition, it also yields MOFs with unique morphologies and particle sizes. Microwave synthesis can produce MOFs with different shapes or sizes by tuning the reaction conditions [59]. Microwave synthesis to give 5-20 nanometer-sized particles of oxides is also known [60]. In this method, a substrate mixture in a suitable solvent is transferred to a Teflon vessel, sealed and placed in the microwave unit, and heated for the appropriate time at the set temperature.

This method follows the approach, where an applied oscillating electric field is coupled with the permanent dipole moment of the molecules in the synthesis medium inducing molecular rotations, resulting in rapid heating of the liquid

phase [61]. Generally, it has many advantages including a small and uniform particle size distribution, good morphological control, and a fast crystallization process. The first MOF synthesized by this method is Cr-MIL-10 [62]. This microwave technique method also has been applied to the synthesis process of MOF which contains trivalent Cr^{3+} , V^{3+} , Ce^{3+} , Fe^{3+} , and Al^{3+} .

Mechano-chemical/ball milling synthesis method. Mechanochemical responses depend on the mechanical energy being directly absorbed by reagents, generally solids, in the process of milling or grinding, similar to ball milling. In this system, friction and collision between balls and reactants are the sources of energy demanded to initiate chemical reactions. Generally, MOFs synthesized by mechanochemical methods possess some distinct characteristics compared to traditional synthesis methods. Some of these are mechanochemical methods that can enhance the purity of MOF products. The grinding action in mechanochemical synthesis can help eliminate impurities and improve the overall purity of the synthesized MOFs [63]. Moreover, it can lead to MOFs with specific particle sizes, such as nanoscale particles or ultrafine powders. Beside this mechanochemical synthesis also offers energy-saving advantages as it avoids the need for high-temperature or solvent-intensive processes; also, the fast reaction kinetics and simplified reaction conditions make them attractive for large-scale production of MOFs [64]. This technique is also environmentally friendly and it has found wide application in various areas, such as metallurgy, mineral processing, construction, and synthesis of organic composites [63].

Solvent-free conditions are applied, which are particularly useful when organic detergent is to be avoided as described in Fig. 6. HKUST-1 was successfully produced by the mechanochemical synthesis method without using a solvent [65]. Besides this, the addition of small amounts of solvents in liquid-supported grinding (LAG) can lead to the acceleration of mechanochemical reactions due to an increase in the mobility of the reactants on the molecular level, and also as a structure-directing agent. Now a day, the extension of the ion method- and liquid-assisted grinding (ILAG) is reported to be largely effective for the picky construction of pillared-layered MOFs [66,67]. However, the mechanochemical method is limited to specific MOF types only and a large amount of product is delicate to gain.

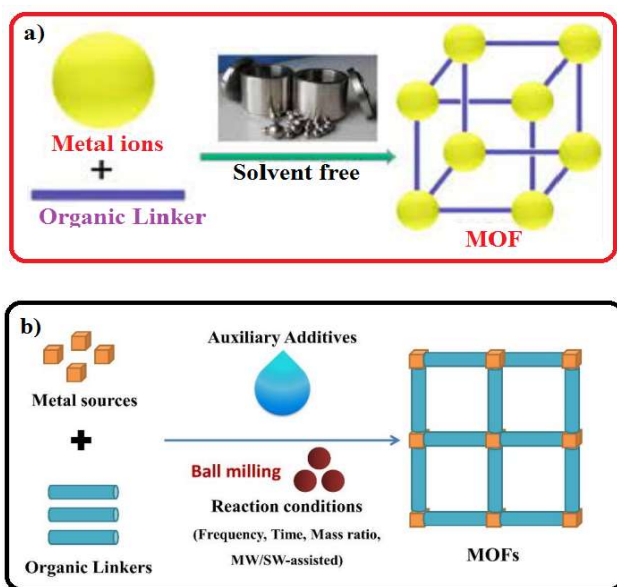


Fig. 6. Mechano-chemical synthesis method a) solvent free b) solvent/additives.

Microfluidic synthesis method. The development of nonstop, brisk, and feasible processes for MOF development would be desirable. In microfluidic, the reaction phase is fitted into the immiscible carrier fluid (oil painting), The micro droplets are generated spontaneously, and also the droplets flow through the inflow channel to form a certain structure of MOFs as shown in Fig. 7 below. This system enables the fabrication of monodisperse nanomaterials with certain properties due to small liquid volumes, rapid-fire mass transfer, and high mixing effectiveness. The synthesis of different MOFs has been also realized by microfluidics using droplets [68] or inflow-fastening administration [69]. Microfluidic synthesis has been employed to produce various types of MOFs with unique characteristics. Here are a few examples of MOFs synthesized using microfluidic techniques, along with their notable characteristics as follows. HKUST-1 MOF microcrystals were synthesized using drop microfluidics. The result revealed that the pore sizes of HKUST-1 could be varied depending on the dimension of the pore precursor [70]. A nonstop flow microfluidic synthesis setup was also applied to realize the synthesis of MOF-composites. It was demonstrated that the change in the MOF reactants in the microchannels resulted in the induction of the defects (mesopores) in a MOF structure.

ZIF-8 (Zeolitic Imidazolate Framework-8) is also a well-known MOF with high stability, porosity, and tunable pore sizes. It exhibits exceptional gas adsorption properties, especially for carbon dioxide (CO₂) capture and storage applications [71]. UiO-66 (University of Oslo-66) is another robust MOF with excellent chemical and thermal stability which is synthesized by microfluidic. It possesses large pore volumes and high surface areas, making it suitable for applications such as gas storage, catalysis, and drug delivery systems [72]. MOF-74 is a class of MOFs that includes different metal ions (*e.g.*, Mg, Ni, Zn) coordinated with organic linkers. These MOFs possess high surface areas, large pore volumes, and excellent thermal stability. They have potential applications in gas storage, adsorption, and catalysis [73].

Spray-drying synthesis method. This synthesis method consists of the atomization of a result containing the MOF precursors into a spray of microdroplets using a two-fluid nozzle. The inner nozzle injects the solution and the outlet compresses the gas. The droplets are thus girdled by the gas at a controlled temperature. The evaporation of the detergent increases the precursor concentrations at the surface while staying for the critical concentration for the reaction to be reached, and the crystallization begins [74]. The MOF's microparticles begin to form inside the droplet, after that, the particles formed are compacted together until all the droplets are faded to form larger particles of MOFs as described in Fig. 8.

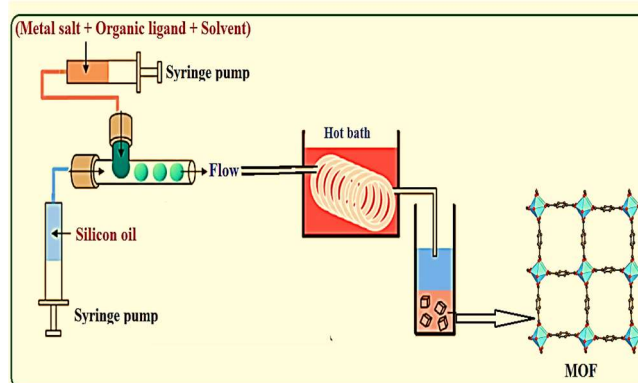


Fig. 7. Systematic description of microfluidic synthesis method. Reprinted by permission from reference [54], Copyright © 2013, Korean Institute of Chemical Engineers.

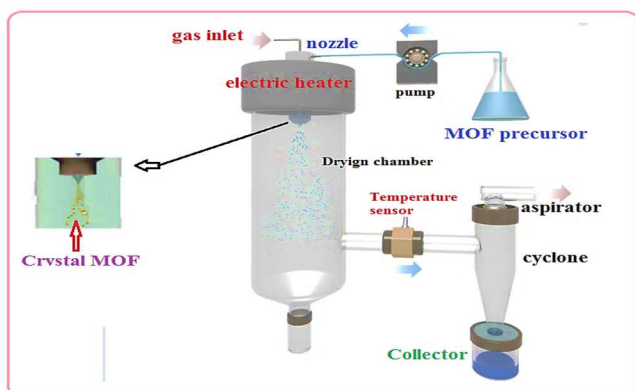


Fig. 8. Spray-drying synthesis method. Reprinted with permission from [75], Copyright ©2017, IOP Publishing Ltd.

Generally, the spray drying method provides a low-cost, rapid, and scalable system for the synthesis and self-assembly of nanoMOFs. Sanchez *et al.* [75] established that the spray drying method is a versatile, low-cost, and rapid procedure enabling not only simultaneous synthesis and assembly of different types of nano-MOFs, with diameters smaller than 5 μm with- without employing secondary immiscible solvent or surfactant. He also proved that the spray-drying procedure enables greater compositional complexity of hollow MOF superstructures. Besides, MasPOCH *et al.* [76] also synthesized various kinds of MOFs including Fe-BTC/MIL-100, UiO-66, and $[\text{Ni}_8(\text{OH})_4(\text{H}_2\text{O})_2(\text{L})_6]_n$ by applying a spray-drying flow-assisted process.

Sono-chemical method. Sonochemistry is a fast-developing branch of chemistry, which is a phenomenon in which the reaction mixture undergoes a chemical change upon application of high-energy ultrasound irradiation from 20 kHz to 10 MHz [77]. The US has been proven superior in terms of simplicity, reduced reaction times, and energy efficiency. In detail, when passing through the reaction mixture, ultrasound irradiation can generate homogenous nucleation centers that lead to decreased MOF crystallization time compared with classic solvothermal or hydrothermal techniques [78]. As described in Fig. 9 below, a substrate solution mixture for a given MOF structure is introduced to a horn-type Pyrex reactor fitted to a sonicator bar with an adjustable power output without external cooling. Formation and collapse of bubbles formed in the solution after sonication termed acoustic cavitation, produce very high

local temperatures ($\sim 5,000$ K) and pressures ($\sim 1,000$ bar) [79] and result in extremely fast heating and cooling rates ($>10^{10}$ K/s) producing fine crystallites [80].

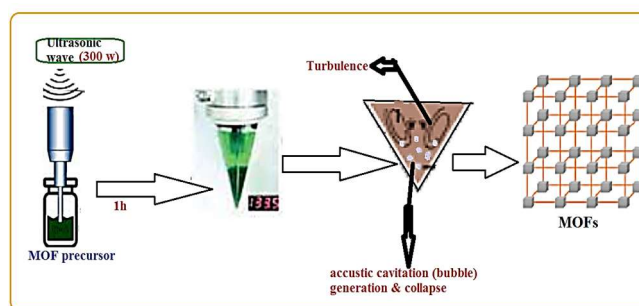


Fig. 9. Sono-chemical synthesis method. Reprinted by permission from reference [54], Copyright © 2013, Korean Institute of Chemical Engineers.

Many researchers reported successful preparation of high-quality MOF-5 [81], ZnBDC [82], HKUST-1 [83], MOF-177 [84], Mg-MOF-74 [85], ZIF-8 [86], and CuTATB-n MOFs [87] crystals *via* a sonochemical method in considerably reduced time compared to conventional methods.

The Characters of Metal-Organic Frameworks

MOFs are hybrid inorganic-organic materials, which means that they have the characters of both inorganic (defined structure and good stability) and organic materials (low density and high flexibility). Generally, the features of MOFs can be concluded as the following three aspects: high surface area and rich porosity, regular and tunable pore texture, and flexibility in surface chemistry.

Tunable porous structures. The properties of porous materials, especially performances in adsorption and separation as well as in catalysis, are tightly related to their porous structures. Strong host-guest interactions within the interior of pores that are the origin of specific functions of materials can only take place when the size and shape of pores meet certain requirements. The combined effect of both inorganic nodes and organic ligands are two basic building blocks of MOFs, and based on their intrinsic geometrical coordination modes, it is possible to get framework structures

with specific topologies by choosing appropriate metal/ligand self-assembly at the molecular level, to achieve regulation over the dimension and shape of apertures to meet the requirement of target applications.

Generally based on the International Union of Pure and Applied Chemistry (IUPAC), porous materials can be classified into three categories according to their pore size (d), which are macroporous materials ($d > 50$ nm), mesoporous materials ($2 \text{ nm} < d < 50$ nm) and microporous materials ($d > 2$ nm). Microporous materials can be further divided into ultra-microporous ($0.7 \text{ nm} < d < 2$ nm) and super-microporous ($d < 0.7$ nm) materials. According to this definition, most of the MOF materials belong to microporous materials, while a few of them are mesoporous.

High surface area. A high surface area is salutary for the exposure of active sites, therefore promoting good physical or chemical properties. MOFs generally retain a BET surface area in the range of $1000\text{-}8000 \text{ m}^2 \text{ g}^{-1}$, which is more advanced than that of traditional previous porous materials like zeolites ($\sim 500 \text{ m}^2 \text{ g}^{-1}$) and active carbons ($\sim 1500 \text{ m}^2 \text{ g}^{-1}$). In 1999 the development of the first stable MOF with a high surface area, that is MOF-5 (the BET surface area is $2320 \text{ m}^2 \text{ g}^{-1}$), the record of the highest surface area of MOF. Experimenters was elevated to $4730 \text{ m}^2 \text{ g}^{-1}$ by UMCM-1 ($\text{Zn}_4\text{O}(\text{BDC})(\text{BTB})_{4/3}$) [88]. It consists of two kinds of ligands, BDC and BTB, with different topologies, bridging with Zn^{2+} cations into a new structure with cage-like micropores and 1D mesoporous channels, distinct from MOF-5 ($\text{Zn} + \text{BDC}$) and MOF-177 ($\text{Zn} + \text{BTB}$). Its volumetric specific surface area reached $2060 \text{ m}^2/\text{cm}^3$, comparable to 3 nm cubic nanoparticles, approaching the adsorption upper limit of solid materials [89].

Functionalized surface. MOF materials have rich components, and the chemical situation of pore surfaces can be deliberately designed by choice of metal nodes and organic ligands to achieve surface functionalization. Generally, the essence bumps in MOFs (such as Al, Fe, Cu, Ni, *etc.*) could serve as Lewis's acid catalysts. Also, ligands with specific functional groups could be used for the synthesis of MOFs to grand the pore surface with acidity/basicity or charges to boost the progress of specific reactions or small molecule adsorption. Besides the pre-design of the pore surface before synthesis, the chemistry of the framework could also be modified after the formation of

MOFs, *i.e.* the post-synthetic modification strategy (PSM) as described above. This strategy is to introduce new functional sites by partial or complete exchange of metal and/or ligands based on the given MOF materials. The metal-exchanged framework maintained its original porous structure, while the pore surface was granted redox reactivity to activate small molecules like NO. For example, by partial substitution of surface ligands in the ZIF-8 framework, the surface hydrophobicity was improved to enhance the hydrothermal stability of the material [90].

Stable MOF

Stable MOF refers to MOF that has stable porosity, framework flexibility, and dynamics when exchanging guest or external stimuli, exhibiting various intelligent properties. Hence, MOFs with high stability usually have strong coordination bonds (thermodynamic stability) or significant steric hindrance (dynamic stability) to prevent the attack of guest molecules or the intrusion of the guest into metal nodes, preventing the hydrolysis reaction that destroys metal coordination bonds [91,92]. When we discuss MOF stability there is chemical stability, which refers to the ability of MOFs to withstand various chemical treatments while maintaining their structural stability and porosity. One key feature that can contribute to a MOF's stability is its coordination bonds' strength and protective groups surrounding those bonds. Several factors can impact the strength of metal-ligand bonds. These factors include the coordination chemistry, structural context, and environmental factors [93]. Efforts to improve MOFs' chemical stability have predominantly centered on mitigating the effects of water (acid, alkali, and salt aqueous solutions) and water vapor [94]. For instance, MOF-5 synthesized from Zn^{2+} is innovative in the research of MOFs, its structure is easy to collapse and gradually decompose after contacting the moisture in the air [95]. This is due to the relatively weak metal coordination bonds, which have poor stability and are very sensitive to water. To understand the water stability of MOF materials, we should understand the factors that affect the stability of MOFs is crucial, such as external factors, metal ions, organic ligands, the metal-ligand coordination case, hole surface hydrophobicity, *etc.*, so that we can reasonably design a stable structural framework [96].

In alkaline waters, the long-term stability of MOFs made of azolate links and ions with low valency stands out, whereas, in acidic conditions, their resistance is only moderate. Due to low-valency metal's intense connection to azolate and hydroxyl's poor interaction with low-valency metals, MOFs are stable in alkaline environments. The metal-organic frameworks (MOFs) containing Zn, Co, and Ni in a bivalent state are notable examples of materials that demonstrate exceptional stability in solutions with high alkalinity. Lu and colleagues have also reported that MAF-X27-Cl (Co) can maintain its crystalline structure after exposure to a 1.0 M KOH solution for seven days [97]. Moreover, the structural integrity and porosity of PCN-601(Ni) remained unaltered even upon immersion in solutions with pH ~14 and saturated NaOH [98]. UiO-66(Zr) also maintained both its crystalline structure and porosity even after being immersed in various saline [99]. In addition, PCN-602 (Ni) also showed remarkable stability in which the affinity between soft metal ions Ni and soft azolate linkers is notably stronger compared with hard liners [100].

APPLICATION OF METAL-ORGANIC FRAMEWORK (MOF) BASED NANOMATERIAL

Veritably lately, important attention has started to explore the synthesis and applications of nanoscale MOFs (nanoMOFs), the particles of which feature at least one dimension at the nanoscale. To date, nano MOFs have shown particular advantages compared to their bulk materials with unique properties, similar as accelerated adsorption/desorption kinetics and accessibility to the internal active sites for enhanced catalysis, suitable sizes for biomedical application, and their assembly to diverse nanostructured materials for energy and membrane separation-related applications. Generally, MOF has unique characteristics such as high surface area, structural diversity, and tolerability. These unique features have led researchers to explore combining MOFs with other functional materials to form novel composites with advanced properties [101]. Metal nanoparticles, polymers, and biomolecules have been combined with MOFs to afford new materials that have demonstrated extraordinary performance (Fig. 10) in the areas of catalysis [102], molecular separations [103],

biomedicine [104-106], energy applications [107-109], sensing [110], plasmonics [111], gas storage [112], controlled guest release [113,114], and protection of biomacromolecules.

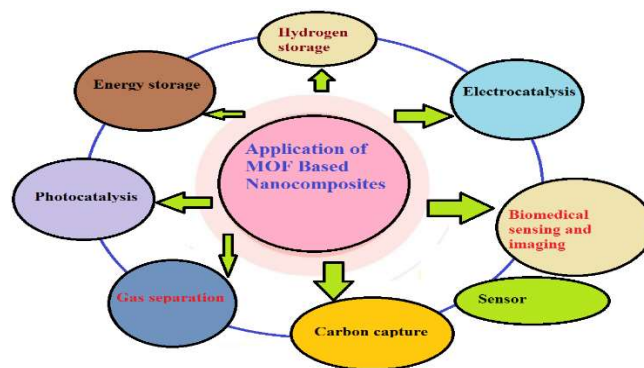


Fig. 10. Various applications of MOF.

Biomedical Application

The unique demitasse structure properties (large specific surface area, suitable sizes, chemical versatility, good biocompatibility, tunable structure, suitable and physiological stability, high porosity, and biodegradability) of MOF have quickly gained further attention in the biomedical field due to their targeted delivery, stability, the controlled release of their loaded contents, and other biological properties [115,116] (Fig. 11). Through a large number of studies, MOFs have been upgraded from the original beneficial delivery and sustained and controlled release to the intelligent direction. These functionalized MOFs can be loaded with therapeutic substances, have programmability, and are more conducive to dealing with complex wounds while achieving coordinated antibacterial, anti-inflammatory, pro-angiogenic, fibroblast generation, and collagen deposition outcomes, effectively improving the safety of treatment [117].

Drug/Cargo delivery. Nano-MOF has become more and more popular, especially in drug delivery. Therefore, MOF materials are excellent candidates to deliver small molecule drugs due to their good biological safety and inherently porous nature. In addition, the biggest advantage of MOFs as a drug carrier is not only the high drug loading but also the long drug release time. The drug carrier refers to a system

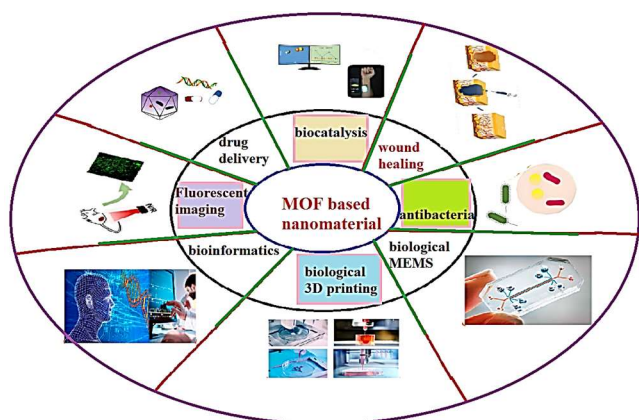


Fig. 11. Diverse application MOF-based nanocomposite in biomedical.

that can change the way the drug enters the body and its distribution in the body, control the release rate of the drug, and deliver the drug to the target organ (Fig. 12). Drug carrier materials play a very important role in the research of controlled-release carriers. The first framework used as a carrier for medication was MIL-100 which was used as a carrier for ibuprofen release [118]. Recently, other frameworks such as UiO-66 [119], MIL-53 [120], and ZIF-8 [121] were made for carrying anti-cancer and anti-inflammatory drugs such as doxorubicin [122], 5-fluorouracil [123] and ibuprofen [124]. In many studies, the level of MOFs and other carriers has been modified using natural and synthetic polymers, including polyacrylic acid (PAA) [125] and polydopamine [126], which has shown good results for drug delivery. Moreover, many researchers studied about drug delivery ability of MOF. An *et al.* first encapsulated the cationic drug procainamide into anionic bio-MOF-1 successfully [127]. The loading of procainamide was 18 wt% and only 20% of the loaded drug was released from bio-MOF-1 after 3 days in neutral PBS. He is also, investigated the drug loading and releasing properties of four bio-MOFs (bio-MOF-1, bio-MOF-4, bio-MOF-100, and bio-MOF-102) [128]. The results showed an initial burst release in all the bio-MOF groups, followed by a progressive release for a long period ranging from 49 to 80 days. Additionally, in 2010, Horcajada and collaborators reported the use of a series of non-toxic porous iron(III)-based nanoMOFs, *i.e.* MIL-53, MIL-88A, MIL-88Bt, MIL-89, MIL-100, and MIL-101-NH₂,

as carriers of antineoplastic and retroviral drugs, including busulfan, azidothymidine triphosphate, doxorubicin or cidofovir, ibuprofen, caffeine, urea, benzophenone 3 and benzophenone 4. Composites of MOF like PEG-modified nano MOFs possess good physiological stability and achieve controlled drug release without a “burst effect” [129].

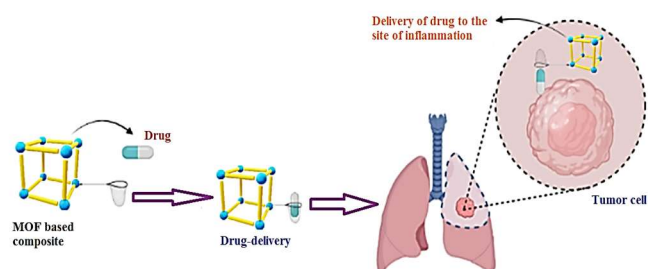


Fig. 12. Representation of drug delivery by MOF-based composite into the tumor cell. Reprinted with permission from [129], Copyright: © 2022, MDPI.

Biomedical imaging. Biomedical imaging technologies have been developed rapidly, which facilitated earlier disease diagnosis and enabled noninvasive monitoring of the therapeutic processes. In recent years, nMOFs have proven to be emerging imaging agents for producing signals or enhancing signal contrast at targeted sites due to their diverse structures, sizes, and metal connecting nodes. As a result, nMOFs can be used to diagnose diseases such as various cancers through optical imaging (OI), X-ray computed tomography (CT), magnetic resonance imaging (MRI), and positron emission tomography (PET). MOF helps in biomedical imaging like CT scans b/c MOFs can be functionalized with high atomic number elements (*e.g.*, iodine or bismuth) to enhance X-ray attenuation, leading to improved contrast in CT imaging. MOFs can be designed to encapsulate paramagnetic metal ions, such as gadolinium (Gd), which generate strong magnetic fields, enhancing the contrast in MRI scans. MOFs can be functionalized with radioactive isotopes, such as gallium-68 (Ga-68) or zirconium-89 (Zr-89), to serve as PET imaging agents. These isotopes emit positrons that can be detected by PET scanners, enabling high-resolution imaging. The nano MOFs can also incorporate different fluorophores to perform intracellular

imaging [130]. Particularly, some Gd^{3+} , Mn^{2+} , and Fe^{3+} -containing nanoMOFs have presented great efficiency for magnetic resonance imaging (MRI), which is a non-invasive imaging technology that detects the direction of nuclear spin in a magnetic field.

Therefore, fluorescent materials were employed to modify the agents for deep tissue imaging and intracellular imaging. For example, Li *et al.* established a new luminescent/magnetic dual-mode imaging method *via* core-shell nanocomposites [131]. This material can be selectively uptake by the KB cell lines *in vitro* and the *in vivo* optical imaging and MRI studies exhibited an obvious contrast in KB tumor at 24 h post-injection. Xia and co-workers also formed an ultrathin La-MOF nanosheet for DNA sensing and imaging, and in the subsequent studies, they synthesized a Dye-P2 + MOF-La complex to monitor adenosine in single cells. Lin *et al.* synthesized a UiO nMOF for a pH-dependent ratiometric sensor, fluorescein isothiocyanate (FITC), which was conjugated to the formed nMOFs covalently [132]. Additionally, Cai *et al.* incorporated indocyanine green (ICG), a near-infrared (NIR) dye, into MIL-100(Fe) nMOFs with a high loading capacity of 40 wt% and a layer of hyaluronic acid (HA) was coated for tumor-targeting [133]. The prepared particles exhibited a strong NIR absorbance, photostability, and high cellular uptake in $CD4^{+}$ MCF-7 cells both *in vitro* and *in vivo* [134].

Antibacterial activity. For antimicrobial applications of MOFs, metal ions, organic ligands, or a combination of them is mainly utilized as an effective biocide to provide antibacterial activity during the stepwise and slower decomposition of MOF skeletons, but these cannot be used repeatedly. There is a different mechanism for anti-bacterial activity in which the MOFs containing anti-bacterial metal ions like Ag^{+} , Cu^{2+} , or Hg^{2+} , release them at the site of action [135], the MOFs act as a wonderful capping agent to prevent aggregation of NPs, their unwanted interaction and stabilizing their atomic dispersions. The linker of the framework which is also an anti-bacterial gets released and then the generation of ROS species (Fig. 13) which most often happens when the NPs are irradiated with light [136,137]. Finally, the MOFs are loaded with anti-bacterial agents which get released over a specific period under the influence of external stimulating factors [138,139].

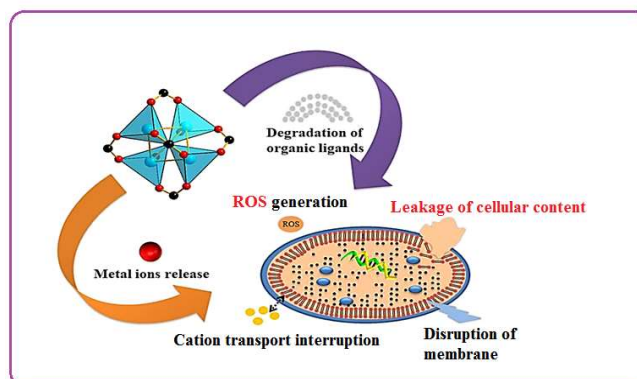


Fig. 13. Anti-bacterial action of MOF. Reproduced with permission from [135], Copyright © 2020. John Wiley & Sons.

The MOFs that are used for treating systemic infections usually comprise more biocompatible metal ions such as Zinc, cobalt, *etc.* *S. aureus* is a gram-positive food-contaminating pathogen that is parasitic on the skin, and GI tract and can cause infection via food and wounds [140]. In many studies, *S. aureus* is taken as an organism of choice for demonstrating the action of the antibacterial system along with the gram-negative *E. coli* which is also part of normal flora. Moreover, antimicrobial agents could also be encapsulated into the pores of MOFs to achieve a controllable release and more lasting antibacterial efficacy [141,142]. Chen *et al.* modified nanoscale and microscale sizes of ZIF-8 crystal films on porous titanium surfaces and showed satisfactory antibacterial effects against *S. mutans* [143]. Wang *et al.* also synthesized ZIF-8/PDA/PS composite membranes by depositing the ZIF-8 crystal layer on a polydopamine (PDA) modified polysulfone membrane. The obtained membranes displayed superior antibacterial activity against *E. coli* with a nearly 99% antibacterial ratio, which might result from the released Zn^{2+} and imidazole ligands from ZIF-8, as well as the produced ROS by composite membranes [144]. Ren *et al.* fabricated HKUST-1/CS film via modification of chitosan (CS) film with HKUST-1. This film exhibited durable antibacterial performance against *S. aureus* and *E. coli* for the slow release of Cu^{2+} . Moreover, HKUST-1/CS could prevent wound infection caused by *S. aureus* and promote skin wound healing, showing great potential as wound dressing [145].

Bio-catalysis. MOFs are ideal candidates for building biomimetic systems because their invariant cavities can generate a high viscosity of biomimetic active centers. In addition, thermally and chemically stable MOFs can be built with a variety of metal clusters. Therefore, the channels of MOFs provide confined pockets, which protect the catalytic centers and enhance substrate specificity. Therefore, porous MOFs are very promising for the immobilization of biomimetic molecular catalysts in the pore surface or space, and thus to realize highly efficient biomimetic catalysis by mimicking certain features of natural enzymes, including active sites, reaction pockets, assistant sites, microenvironment, and transmission channels [146,147]. Besides these, the uniform and well-defined structures of biomimetic MOFs offer a comprehensive understanding of the structure-function relationship. Biomimetic MOFs present the following characters such as uniform dispersion of active sites, tunable hydrophobic and hydrophilic pore nature, collaborative microenvironment, and confined catalytic reaction pockets and transmission channels. Zhang *et al.* reported a nanometric MIL-100, which performed the intrinsic peroxidase-like catalytic activity, for ascorbic acid colorimetric sensing [148]. The prepared nMOFs catalyzed the oxidation of different peroxidase substrates by H_2O_2 and caused the obvious color change of the solution. Wu and coworkers also synthesized a metalloporphyrin-bioMOF as a tri-component biomimetic catalyst platform consisting of sandwich-type polyoxometallate and N-hydroxy phthalimide [149-151]. The studies on the aerobic oxidation of ethylbenzene showed that the formed nanoparticles could immensely enhance the oxidation reaction under mild conditions. Ma *et al.* first reported the successful immobilization of micro peroxidase-11 (MP-11) into the mesoporous MOFs and the MP-11@Tb-mesoMOFs showed a better catalytic capacity compared with the previous MP-11 [152]. A catalytic ZIF-8 was also synthesized with two enzymes immobilized, including FITC-labelled glucose oxidase (GOx) and horseradish peroxidase (HRP), for detecting glucose in cells. The nanocomposite displayed high catalytic efficiency, excellent selectivity, and thermal stability [153].

Photocatalytic Degradation

Organic pollutants in water, as a devastating problem in

environmental chemistry, have raised many concerns. Photodegradation of organic pollutants is considered an ideal strategy to solve the issue, which usually involves O_2 as the oxidizing agent to degrade organic pollutants to CO_2 , water, and other inorganic species (Fig. 14). In the first step of the photocatalytic process, pollutants are transported from the environment to the surface of the photocatalyst where oxidation-reduction reactions take place. Photogenerated electrons in the CB and holes in the VB force this response to do so. Also, the products are desorbed and returned to the liquid phase. To generate electron-hole pairs, the energy of the photons must be equal to or exceed the band gap of the photocatalyst [154]. In the photodegradation of dyes, materials such as oxides, metal salts, or chalcogenides, including their composites were described, although recently MOFs-based nanocomposites have been willingly utilized [155]. The large surface area, a wide selection of metallic centers and organic linkers, as well as the possibility to control morphological properties, make MOFs excellent potential for photocatalysts [156].

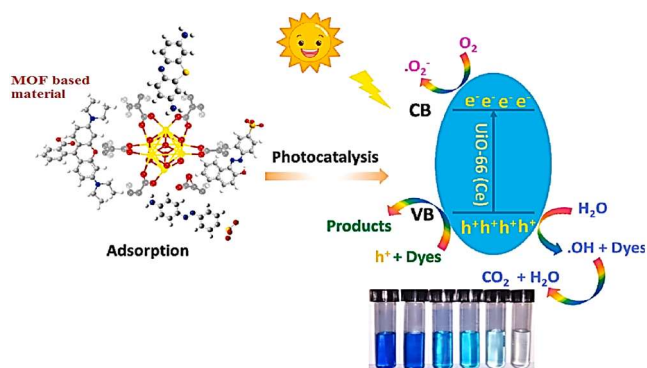


Fig. 14. Photocatalytic degradation mechanism of dye by using MOF-based material.

Especially, MOF-derived materials, such as porous metal oxides, metal sulfides, and their composites (mostly combined with carbon materials) can serve as highly potential photocatalysts due to the merits of high stability, excellent optical absorption/mass transfer, and improved electron-hole separation. Table 1 below shows some of the MOFs-based composites that have been used in various photocatalytic activities.

Table 1. Photocatalytic Degradation of Different Pollutants by MOF-based Nanocomposites

No.	MOFs-Based composites	Band gap energy (eV)	Target pollutant	Ref.
1.	ZIF-8	2.98	MB	[157]
2.	g-C ₃ N ₄ /MIL-101(Fe)	2.05	RhB	[158]
3.	UiO-66-NH ₂	2.63	Acetaminophen	[159]
4.	g-C ₃ N ₄ /MIL-53(Fe)	2.51	Cr(VI)	[160]
5.	Co-Fe-MOF	2.11	RhB	[161]
6.	MIL-125	3.07	Nitrobenzene	[162]
7.	MOF-5	–	RhB	[163]
8.	TiO ₂ /magnetic MIL-101(Cr)	1.61	Acidic red 1	[164]
9.	Fe/Ce-MOF-3	1.75	MO	[165]
10.	Ag ₃ PO ₄ /Ti-BDC/g-C ₃ N ₄ -x	2.9	MO	[166]
11.	CdSe QDs@ Fe-MOF	–	RhB	[167]

Where MB is methyl blue, RhB is rhodium blue and MO is methyl orange.

Sensor

Metal-organic frameworks (MOFs) as described above, which are constructed by the self-assembly process of metal cations or metal clusters and organic ligands have increased attention due to possessing large surface areas, high porosity, tunable structural, and robust thermal stability. Therefore, due to these properties' MOFs based composites have been also employed to be one of the leading nominees for sensing different components, and different MOFs have been synthesized as detecting platforms for special analytes such as inorganic ions, gases, organic small molecules, explosives, temperature, humidity, antigens, and protein. The major types of sensors are electrochemical and optical (fluorescent) sensors based on MOF composites are discussed below.

Electrochemical sensor. Metal-organic frameworks (MOFs) grounded nanocomposites are an attractive porous material with exceptional specific surface area, tunable pore size, and abundant active sites that can be exploited as catalysts for electrochemical discovery [168,169]. They show great potential in the preparation of electrochemical sensors, which extends their application to the detection of analytes in different industrial fields, including environmental and biomedical fields, among others [170, 171]. The mechanism is when the pore structure of carbon paste electrode-modified MOFs compound can allow the analyte to be pre-concentrated from the bulk solution onto the electrode surface, which helps to increase the selectivity of the analyte [172]. For illustration, Co-based metal-organic

coordination polymer-modified carbon paste electrodes are developed to analyze the electrocatalytic performance of redox glutathione [173]. This constructed compound shows excellent electrocatalytic oxidation-reduction and high selectivity of glutathione (Figs. 15A, B, C). Also, MOF/graphene (or graphene oxide) mixes have been developed in several electrochemical sensing applications. A copper-based MOF is also proposed by combining with graphene for electrochemical sensing of H₂O₂ and ascorbic acid (Figs. 15D, E, F) [174].

Due to the hydrogen bond between Cu-MOF and graphene, p-p stacking, and Cu-O coordination, the synthesized nanocomposites exhibit high stability and good anti-interference properties to detect H₂O₂ and ascorbic acid in various carbohydrates. Deng and coworkers also prepared UiO-66/mesoporous carbon (MC) composite *via* the hydrothermal method for the first time to recognize dihydroxybenzene isomers (DBIs) of phenolic compounds [176]. The result suggested that when the mass proportion of UiO-66 and MC was 1:2, the peak currents and peak-to-peak separations of DBIs became a maximum value. The semicircle of MC/GCE and UiO-66/MC/GCE is not clear thus the electron transfer capability of UiO-66 is developed immensely after modifying MC. Furthermore, to detect tryptophan (Trp), MIL-101(Fe) with the exterior modified by silver nanoparticles (AgNPs) was put on the surface of a glassy carbon electrode (AgNPs/MIL-101/GCE) [177]. The

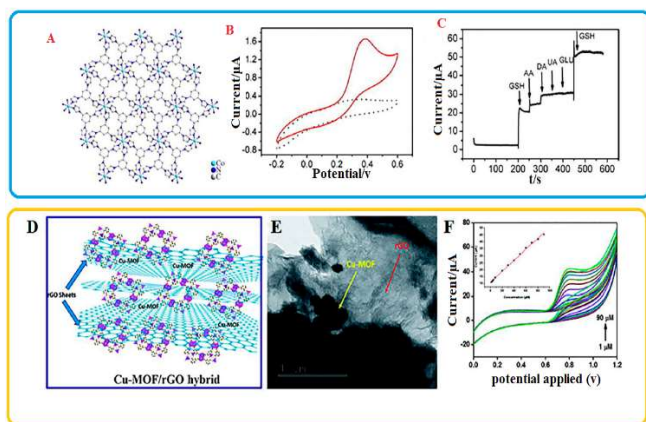


Fig. 10. (A) Illustration of the structure of metal-organic coordination polymers with 1,3,5-tris (1-imidazolyl) benzene and Co^{2+} (Co-MOCP), CVs (B), and interference test (C) of the Co-MOCP/carbon paste electrode in the different solution [174]. Reprinted with permission, Copyright © 2014, Elsevier. Schematic structure (D), transmission electron microscope (TEM) images (E), and CV curves at different nitrite concentrations (F) of the Cu-MOF/rGO hybrid [175] Reprinted with permission, Copyright ©2016, RSC.

combination of the great specific surface area of MOF and the high electrical conductivity of silver nanoparticles makes AgNPs/MIL-101 an excellent sensor for this purpose with $0.14 \mu\text{M}$ ($\text{S/N} = 3$) detection limit in optimum $\text{pH} = 2.4$. The AgNPs/MIL-101/GCE increased the electron transfer between the electrode and the solution leading to a more sensitive current response in the oxidation of Trp under the selected experimental conditions.

Based on the importance of sensing cocaine in clinical diagnostics, Su and others began to AuNCs@521-MOF and examined its efficiency as an electrochemical sensor for detecting cocaine [178]. The excellent electrochemical activity of Au NCs and the high special surface area of the 2D nanosheets, as well as the exceptional chemical and thermal stability, increase the attractive nature of this framework. From electrochemical data, the AuNCs@521-MOF-based aptasensor exhibited better detection efficiency for cocaine compared with the pristine 521-MOF. There are many MOF composites are reported for electrochemical detection of glucose with a good linear range, sensitivity, and detection limit like Ni-BDC MOF [179], $\text{Cu}_2\text{O}@ZIF-67$

[180], ZIF- N_2 [181], Cu-MOF [182], $\text{Ag}@TiO_2@ZIF-67$ [183], $\text{Ag}@ZIF-67$ [184], Ni-BDC- NH_2 [185]. In addition, Zhang *et al.* also reported a hydrothermal synthesis of hybrid material [polyoxometalate based-MOF (POMOF)/rGO] has been proposed to detect dopamine electrochemically (Fig. 16) [186]. These sensor-promoted electron transfer, available active sites, open channels, and aromatic planes in the hybrid material provided a wider linear detection range from 1×10^{-6} to 2×10^{-4} M with a lower detection limit of 80.4×10^{-9} M ($\text{S/N} = 3$) and sensitivity of $0.373 \text{ mA} \times 10^{-3} \text{ M}^{-1} \text{ cm}^{-2}$ during 100 reusability cycles with 21% of performance reduction.

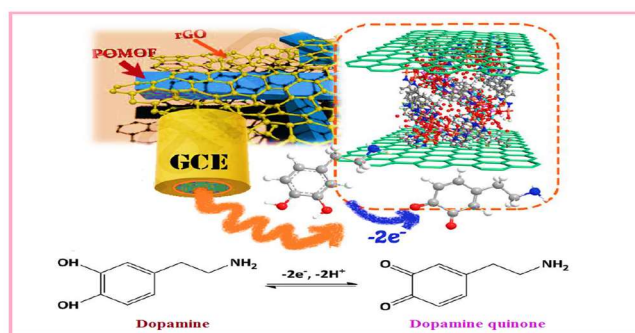


Fig. 16. Schematic representation of the producing and detecting of DA in POMOFs/rGO. Adapted with permission from [187], Copyright © 2017. John Wiley & Sons.

$\text{UiO-66-NH}_2@PANI$ was synthesized during polymerizing the conductive polyaniline (PANI) polymer around the UiO-66-NH_2 via using aniline as monomer due to good stability and the presence of amine group to detect toxic Cd^{2+} metal ion [188]. They used cyclic voltammetry (CV) and electrochemical impedance spectroscopy (EIS) to assess the characteristics of modified electrodes [$\text{UiO-66-NH}_2@PANI/\text{GCE}$]. Based on the result obtained curves, the CV response of $\text{UiO-66-NH}_2@PANI$ modified GCE exhibited the biggest current signal, demonstrating that the cooperation of UiO-66-NH_2 and PANI accelerates the electron transfer and improves the electrochemical sensitivity.

Fluorescent sensor. The development of fluorescent sensors for the recognition and sense of the biological and environmental analyte has drawn continuous interest in fields

of chemistry, materials, and biological and environmental sciences due to the low cost, simple operation, high sensitivity and specificity, real-time monitoring, and short response time [189]. Upon interactions with the analyte, the fluorescence intensity and/or fluorescence band shift of the sensors change and the analyte may be detected qualitatively and quantitatively [190]. Lately, fluorescence techniques have been widely used to detect changes in the concentration of analytes in a very narrow space. The mechanism is typical, a system (molecule or atom) is excited by irradiation at a particular wavelength of light. The irradiated species earn energy by absorbing a photon and entering an agitated state. Then by losing this energy, the system can relax by emitting a photon. The difference in wavelength between absorption and emission bands has been widely applied in the development of various fluorescent sensors since it enables analysis with high sensitivity [191]. Generally, the photoinduced electron transfer (PET), electronic energy transfer (EET), Förster resonance energy transfer (FRET), inner filter effect, and other methods have been used to develop fluorescence-based sensors [192] and some are described in Fig. 17.

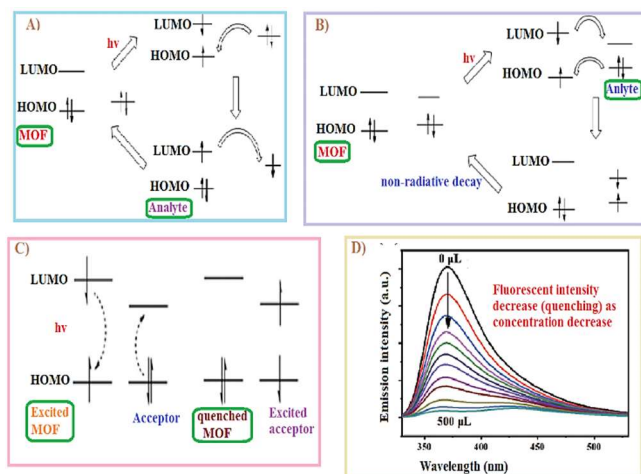


Fig. 17. a) PET process with the participation of the fluorophore and an external molecular orbital, b) EET process of the fluorophore and an external molecular orbital, c) Molecular orbital schematic illustration for resonance energy transfer (RET) [193], and d) representation of fluorescent quenching up on binding with the analyte. Reprinted with permission from [193], Copyright © 2022, Tsinghua University Press.

Extraordinarily, the fluorescent properties of MOFs can be very sensitive to external stimulations, making them well-suited for fluorescent sensing [194-196]. This material has the advantage of high porosity, and the sensitivity of MOF-based fluorescent sensors could be improved under the possible preconcentration of analytes [197]. Therefore, fluorescent MOFs based composites have been successfully utilized to detect proteins, enzymes, nucleic acid, small biomolecules, antibiotics, small organic molecules, and inorganic ions. Some of the reported findings are discussed as follows. There are many MOF composites are developed for the detection of cations like UiO-66(OH)₂ with porphyrin-based MOF PCN-224 for Cu²⁺ [198], curcumin@MOF-5 composites for Al³⁺ ions by PET process [199], (NTU-9 nanosheets, Tb-MOFs, and dye@Zr-MOFs) for Fe³⁺ through the PET and/or IFE process [200-203], Cd(II)-MOFs for Cr³⁺ detection [204], NH₃ plasma-functionalized UiO-66-NH₂ for the detection of U(VI) by static quenching [205]. On the other hand, a Tb(III)-functionalized Zn-MOFs for fluorometric detection of PO₄³⁻ [206], (UiO-68-ol, NH₂-MIL-53(Al), oxime-Eu(III)/UiO-67 for ClO₂⁻ via energy transfer [207-209], RhB/UiO-66-N₃) for H₂S [210], RhB/Cd-MOFs for 4-nitroaniline [211] was developed.

Qin *et al.* also developed a two-dimensional ultrathin Cd-MOF/Tb³⁺ fluorescent nanosheet to detect cefixime antibiotics via PET and IFE [212]. MOFs with intrinsic fluorescence can be additionally used as electron or energy donors to develop a biosensor for DNA detection. Ln-MOFs were developed for detecting miRNA *via* FRET [213]. The researcher also developed the fluorescence proximity assay for the detection of prostate-specific antigen (PSA) by using MOF@AuNP@graphene oxide as the nano quencher [214]. The general function of MOF-based composite as a fluorescent sensor is described in Table 2 below.

Hydrogen Storage

MOFs based composites can store hydrogen due to the large available surface rather than other materials [224]. Their hybrid metallic and molecular composition allows for several adjustments, such as the functionalization of possible ligands and their storage under variable temperatures [225]. Thus, MOFs have also come veritably promising in replacing noble metals during hydrogenation syntheses as Pt, the most generally used metal to this end, is

Table 2. Various MOF-based Nanocomposites Fluorescent Sensors for the Detection of Different Analyte

Sensor	Detected analyte	LOD	Linear range	Ref.
1.[Fe(II)-MOF-NPs]	Hg ²⁺	1.17 nM	1.0 nM-1.0 μM	[215]
2. [NH ₂ -MIL-125(Ti)]	Pb ²⁺	7.7 pM	0-11 nM	[216]
3. Eu(III)@UMOFs	Hg ²⁺ , Ag ⁺ and S ²⁻	-	-	[217]
4. M-ZIF-90	CN ⁻	2 μM	0-0.1 mM	[218]
5. RhB@Cd-MOFs	4-Nitroaniline	43.06 μM	0-0.054 mM	[211]
6. Zn-MOF)	Parathion	1.95 μg l ⁻¹	5 μg l ⁻¹ -1 mg l ⁻¹	[219]
7. ZnO@ZIF-8	Formaldehyde	-	10-200 ppm	[220]
8. Zn-MOFs	Ofloxacin	0.52 μM	0-0.0215 mM	[221]
9. Eu-MOF@Fe ²⁺	BrO ₄ ⁻	3.7 μM	0-0.2 mM	[222]
10. UiO-66-NH ₂ @Ru)	Melamine	0.27 μM	0.27-110 μM	[223]

expensive and, indeed when compared to MOFs, shows lower yields in hydrogen trapping [226]. Many researchers have reported the use of hydrogen as a fuel and its storage in metal-organic framework materials such as NaNi₃(OH)(5-sulfoisophthalate)₂, Zn₂(2,5-dihydroxyterephthalate) Ni₁₂(OH)₁₂[(HPO₄)₈(PO₄)₄], HCu[(Cu₄Cl)₃(1,3,5benzenetris tetrazolate)₈]-3.5HCl. Generally, MOF-based nanomaterials, as they possess pores that serve as “gas pockets”, hold hydrogen [227] atoms for synthesis as described in Fig. 18 below.

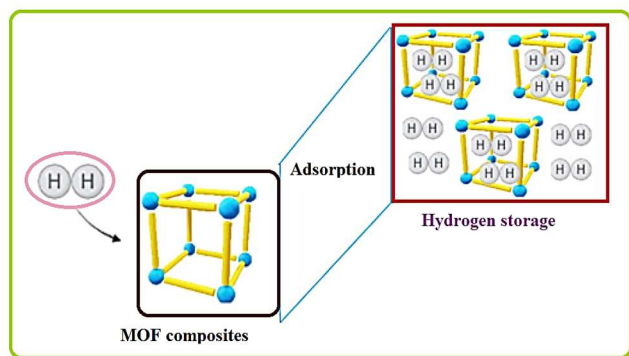


Fig. 18. Metal-organic frameworks (MOFs) used for hydrogen storage which are captured by adsorption. Reprinted with permission from [129], Copyright: © 2022, MDPI

Adsorption

Adsorption is a natural phenomenon where one or further components of a fluid mixture are transferred on the surface

of a solid material by physical or chemical interaction, bringing a concentration variation compared to the adjacent phases. These processes are generally employed in the industrial environment for both compound separation and wastewater treatment. It is characterized by numerous attractive features, including cost-effectiveness, ease of design and operation, and resistance to toxic substances [228]. Adsorption is the most prominent application of MOFs for the removal of emerging contaminants from wastewater. High specific surface area and porosity, structurally flexible, customizable, and photometric, which make them useful in multiple areas of MOFs enhance the ability to adsorb persistent pollutants from aqueous media. More specifically, they have been employed in the removal of excess biological compounds, antibiotics, pesticides, gases, and other toxic pollutants, similar to heavy metals [229]. Researchers reported the adsorption process of organophosphate compounds used as herbicides, glufosinate (GLUF), glyphosate (GLY), and bialaphos (BIA) via MOFs [230, 231]. They are hard to remove due to their high solubility and polarity. So, the adsorption process described made use of the magnetic properties of these MOFs, their high structural porosity, available surface area, and the possibility of compounds being quickly bound to the metallic center [232].

A nanostructured Fe-Co-based metal-organic framework (MOF-74) adsorbent was synthesized by Sun *et al.* to extract arsenic from water with maximum adsorption capacities toward As(V) and As(III) are 292.29 and 266.52 mg g⁻¹, respectively [233]. Additionally, bicomponent zirconium(IV) benzene-tricarboxylate Zr(BTC) post-synthetically with dodeca-tungstophosphoric acid (HPW/Zr)

was developed and used as an effective adsorbent for Benzothiophene with adsorption capacities were to be 238 mg g⁻¹ for Zr(BTC) and 290 mg g⁻¹ for HPW (1.5)/Zr(BTC) [234]. Yin *et al.* also produced hierarchical porous UiO-66 (HP-UiO-66) materials which showed an excellent adsorption behavior of uranium. Moreover, MIL-101(Fe)@PDopa@Fe₃O₄ for malachite green (MG) and methyl red (MR) [235], P₂W₁₈@MIL-101(Cr) for methyl orange (MO), Rhodamine B (RhB), and methylene blue (MB) organic dyes adsorption was developed [236].

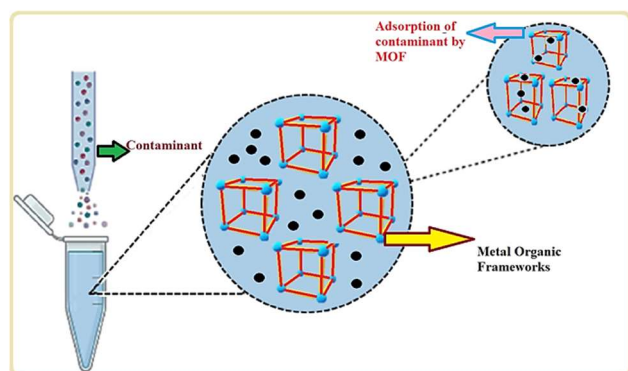


Fig. 19. Pollutant adsorption on the surface of metal-organic frameworks (MOFs), where the contaminant particles can bind to the material, leaving a pollutant-free aqueous medium. Reprinted with permission from [129], Copyright: © 2022, MDPI.

Carbon Capture

The CCS technology (carbon capture and storage) is

proposed as one of the ways of stabilizing the concentrations of CO₂ in the air, apart from reducing the energy intensity of processes and the intensity of carbon dioxide emission [237]. The aim of carbon capture (CC) is to address emissions mostly coming from the burning of fossil fuels in the energy production and transport sectors with the following; storage, for example, in the geological environment (depleted air/gas/water reservoirs, other geological structures), thus mitigating inevitable emissions [238]. The next step [239] of the CC concept is to develop approaches to how to use CO₂ as source material for other substances, thus transforming waste products of human activities into a resource for other products (carbon capture, storage, and utilization (CCSU)).

Metal framework (MOF) which has three-dimensional, microporous materials with crystalline structures is a promising group of adsorbents for CC [240]. Therefore, by changing the structure of ligands and metal atoms, several MOF structures have been created with designed pore and channel sizes from angstroms to nanometers, large surface areas, and a wide variety of structures responsible for CO₂ sorption, and large void volumes for storage [241]. Generally, the interaction(s) between the MOF and CO₂ adsorbate molecules play a critical role, as increasing the strength of such interactions augments the material's CO₂ uptake capacity, especially at low loading pressure. The methods employed to increase these interaction strengths stem from tailoring the frameworks' chemical and physical properties. To date, many reports focus on the study of CO₂ capture and increasing the capacity in MOFs as described in Table 3 below.

Table 3. Performance of MOF-based Nanomaterial as Electrochemical Sensor

Adsorbent	Capacity (mmol g ⁻¹)	T ⁰ (K)	Pressure (bar)	Ref.
HKUST-1	4.51	298	-	[242]
HKUST-1/GO	0.98	298	1	[243]
CuBTC@1%GO	8.90	273	1	[244]
MWCNTs@CuBTC	3.26	298	1	[245]
UiO-66-aminoalcohol	11.6	308	20	[246]
Bio-MOF-11	4.1	298	1	[247]
NH ₂ -MIL-53	2.3	303	5	[248]
Mg-MOF-74	5.4	296	0.1	[249]
MIL-102	3.1	304	30	[250]
CNT@Cu ₃ (BTC) ₂	595	298	18	[251]

Energy Storage

The energy crisis has reappeared as a severe social issue that is hot growth and eventually endangering human survival [252]. Therefore, the global consumption of sustainable and alternative energy resources is growing relentlessly alongside a vigorous worldwide upsurge in concern regarding environmental issues such as global warming and inappropriate climate change. Energy storage and conversion technologies that are renewable, safe, clean, and long-lasting have become a hot research topic [253]. Advances in the development of clean, renewable, safe, and practical energy storage systems such as batteries and supercapacitors [254-256] have attracted widespread interest from the scientific community. A supercapacitor, known as an energy storage device with a high-power density, exhibits excellent rate performance and long cycle life. Due to the increase in energy storage and conversion requirements, these devices have received considerable attention and have become the main device for the further development of power supplies. SCs are presently found in consumer electronics, power supply, voltage stabilization, microgrids, renewable energy storage, energy harvesting, streetlights, medical applications, military, and automotive applications [257].

The SC is composed of high surface-area electrodes (such as anode and cathode), an electrolyte (for example, aqueous medium/organic medium), and a separator. The electrode is an important element that controls the performance of the SC. Therefore, the construction of ultrahigh-performance SC electrodes includes various serious characteristics such as high specific surface area, extraordinary conductivity,

stability based on temperature, optimizing the distribution of pore size, appropriate processing, adequate corrosive resistance, and cost efficiency [258]. Primarily, the selection of appropriate materials and optimizing the electrode design are vital approaches to converting SCs into more energy-efficient energy storage devices than secondary ion batteries [259-261].

Metal-organic skeleton (MOF) materials are characterized by large pore volume, high specific surface area, low densities, good thermal stability, ordered crystal structure, and abundant active metal centers [262], which show excellent capacitive performance when applied to the SC electrode materials. Generally, there are different MOF-based nanocomposites developed for a super capacitor as energy storage. For instance, rGO/HKUST-1 [263], Ni-MOF/GO composite electrode performed an Sc application [264].

The SC is composed of high surface-area electrodes (such as anode and cathode), an electrolyte (for example, aqueous medium/organic medium), and a separator. The electrode is an important element that controls the performance of the SC. Therefore, the construction of ultrahigh-performance SC electrodes includes various serious characteristics such as high specific surface area, extraordinary conductivity, stability based on temperature, optimizing the distribution of pore size, appropriate processing, adequate corrosive resistance, and cost efficiency [258]. Primarily, the selection of appropriate materials and optimizing the electrode design are vital approaches to converting SCs into more energy-efficient energy storage devices than secondary ion batteries [259-261].

Table 4. MOF Composite is Used as a Supercapacitor (Energy Storage)

Electrode material	ED (Wh/kg)	PD (W/kg)	SC (F/g)	Ref.
rGO/ZIF-67	-	-	210	[265]
Ni-Co LDH ZIF-67	68	594.9	1265	[266]
MOF-74	-	-	797	[267]
Mn-Co-ZIF	54.15	324.9	1763	[268]
GO/Mo-MOF	55	400	617	[269]
rGO-Ni-MOF	37.8	227	758	[270]
Fe ^{III} -MOF-5	82.5	675	326	[271]
2D Co-MOF	27.3	22.9	1055.3	[272]

Where ED: energy density, PD: power density, and SC: specific capacity

Metal-organic skeleton (MOF) materials are characterized by large pore volume, high specific surface area, low densities, good thermal stability, ordered crystal structure, and abundant active metal centers [262], which show excellent capacitive performance when applied to the SC electrode materials. Generally, there are different MOF-based nanocomposites developed for a super capacitor as energy storage. For instance, rGO/HKUST-1 [263], Ni-MOF/GO composite electrode performed an Sc application [264].

CONCLUSION AND FUTURE PERSPECTIVE

At this time, MOFs are considered a new member of porous materials and unique advantage over traditional porous materials that recently have attracted all attention to materials chemistry. These are crystalline porous materials in which the metal is fixed in place to fabricate a porous and rigid geometry and uses various bridging ligands. Generally, novel structures and materials with remarkable features have been meant to be created through the synthesis of nano-sized MOF, and improvements have been made in this area, expanding its range through modification. There are many synthesis methods available other than a conventional method like mechano, sono, electro-chemical synthesis, and microwave-assisted syntheses that are just developing, and also room temperature synthesis is the best method now a day. This is due to the method focuses on the direct preparation of MOFs under more sustainable conditions and the harmful organic solvents are replaced partly by water. These techniques can be exploited for some materials, which leads to the production of compounds with various features and particle sizes. As there is a large amount of flexibility in tailoring the structural framework and functionalization, MOFs will likely assume a substantially more significant role in the future to achieve an elevated level of application research in the field of MOFs is expanding quickly in academia and industry. Therefore, there is no doubt that MOFs are prepared in a simple, easy, green, and low-cost way and large-scale production which is applicable as adsorption, catalysts, sensors, electrochemical charge storage, drug delivery systems, *etc.*

For future direction, the following listed ideas are key

aspects that need to be considered in the future: Avoiding harsh processing conditions during synthesis such as high temperature and pressure, which would reduce capital and operating costs and alleviate safety concerns. Developing lanthanide (Ce, Th, *etc.*) incorporating MOF provides better performance for different applications especially fluorescent and electrochemical sensors. The developing of nano-MOF treatments with high biological safety would be also the focus of a futuristic approach to the synthesis of nano-MOFs, which considerably helps the integration of their advantages and enhances the performance of the resulting composites about membrane separation, energy, and catalysis.

REFERENCES

- [1] H. Gleiter, *Acta Mater.* 48 (2000) 1.
- [2] L.G. Qiu, Z.Q. Li, Y. Wu, W. Wang, T. Xu, X. Jian, *Chem. Commun.* 31 (2008) 3642.
- [3] B.S. Barros, O.J. de Lima Neto, A.C. de Oliveira Fros, J. Kulesza, *Chemistry Select* 3 (2018) 7459.
- [4] V.F. Cheong, P.Y. Moh, *Mater. Sci. Technol.* 34 (2018) 1025.
- [5] H. Furukawa, K.E. Cordova, M. O’Keeffe, O.M. Yaghi, *Science.* 341 (2013) 1230444.
- [6] S.R. Batten, N.R. Champness, X.M. Chen, J. Garcia-Martinez, S. Kitagawa, L. Öhrström, M. O’Keeffe, M.P. Suh, J. Reedijk, *Pure Appl. Chem.* 85 (2013) 1715.
- [7] M. Mon, R. Bruno, J. Ferrando-Soria, D. Armentano, E. Pardo, *J. Mater. Chem. A* 6 (2018) 4912.
- [8] J.R. Li, J. Sculley, H.C. Zhou, *Chem. Rev.* 112 (2012) 869.
- [9] H.J. Buser, D. Schwarzenbach, W. Petter, A.J.I.C Ludi, *Inorg. Chem.* 16 (1997) 2704.
- [10] E. Sharmin, F. Zafar, *IntechOpen.* (2016)
- [11] K. Sumida, D.L. Rogow, J.A. Mason, T.M. McDonald, E.D. Bloch, Z.R. Herm, T.H. Bae, J.R. Long, *Chem Rev.* 112 (2012) 724.
- [12] N.L. Rosi, M. Eddaoudi, J. Kim, M. O’Keeffe, O.M. Yaghi, *Angew. Chem. Int. Ed.* 41 (2002) 284.
- [13] Z. Ni, R.I. Masel, *J. Am. Chem. Soc.* 128 (2006) 12394.
- [14] A.A. Tehrani, V. Safarifard, A. Morsali, G. Bruno, H.A. Rudbari, *Inorg. Chem. Commun.* 59 (2015) 41.
- [15] M. Klimakow, P. Klobes, A.F. Thünemann, K.

- Rademann, F. Emmerling, *Chem. Mater.* 22 (2010) 5216.
- [16] L. Chen, Y. Shen, J. Bai, C. Wang, *J. Solid State Chem.* 182 (2009) 2298.
- [17] L. Garzon-Tovar, M. Cano-Sarabia, A. Carné-Sánchez, C. Carbonell, I. Imaz, D. Maspoch, *React. Chem. Eng.* 1 (2016) 533.
- [18] H. Al-Kutubi, J. Gascon, E.J. Sudhölter, L. Rassaei, *Chem Electro Chem.* 2 (2015) 462.
- [19] Z. Peng, Z. Jiang, X. Huang, Y. Li, *RSC Adv.* 6 (2016) 13742.
- [20] L.L. Wu, Z. Wang, S.N. Zhao, X. Meng, X.Z. Song, J. Feng, S.Y. Song, H.J. Zhang, *Chem. Eur. J.* 22 (2016) 477.
- [21] G. Lu, O.K. Farha, L.E. Kreno, P.M. Schoenecker, K.S. Walton, R.P. Van Duyne, J.T. Hupp, *Adv. Mater.* 23 (2011) 4449.
- [22] S. Qiu, M. Xue, G. Zhu, *Chem. Soc. Rev.* 43 (2014) 6116.
- [23] M. Dinca, J.R. Long, *J. Am. Chem. Soc.* 127 (2005) 9376.
- [24] D. Britt, H. Furukawa, B. Wang, T.G. Glover, O.M. Yaghi, *PNAS.* 106 (2009) 20637.
- [25] G. Férey, C. Serre, T. Devic, G. Maurin, H. Jobic, P.L. Llewellyn, G. De Weireld, A. Vimont, M. Daturi, J.S. Chang, *Chem. Soc. Rev.* 40 (2011) 550.
- [26] L. Pan, D.H. Olson, L.R. Ciemnomolonski, R. Heddy, J. Li, *Angew. Chem. Int. Ed.* 45 (2006) 616.
- [27] R. Matsuda, T. Tsujino, H. Sato, Y. Kubota, K. Morishige, M. Takata, S. Kitagawa, *Chem. Sci.* 1 (2010) 315.
- [28] P. Horcajada, R. Gref, T. Baati, P.K. Allan, G. Maurin, P. Couvreur, G. Férey, R.E. Morris, C. Serre, *Chem. Rev.* 112 (2012) 1232.
- [29] E.D. Bloch, W.L. Queen, S. Chavan, P.S. Wheatley, J.M. Zadrozny, R. Morris, C.M. Brown, C. Lamberti, S. Bordiga, J.R. Long, *J. Am. Chem. Soc.* 137 (2015) 3466.
- [30] J.L. Wang, C. Wang, W. Lin, *ACS Catal.* 2 (2012) 2630.
- [31] Y. Cui, Y. Yue, G. Qian, B. Chen, *Chem. Rev.* 112 (2012) 1126.
- [32] J. Heine, K. Müller-Buschbaum, *Chem. Soc. Rev.* 42 (2013) 9232.
- [33] Y. Cui, B. Chen, G. Qian, *Coord. Chem. Rev.* 273 (2014) 76.
- [34] Z. Hu, B.J. Deibert, J. Li, *Chem. Soc. Rev.* 43 (2014) 5815.
- [35] J. Liu, L. Chen, H. Cui, J. Zhang, L. Zhang, C.Y. Su, *Chem. Soc. Rev.* 43 (2014) 6011.
- [36] K. Leus, Y.Y. Liu, P. Van Der Voort, *Catal. Rev.* 56 (2014) 1.
- [37] F. Song, C. Wang, J.M. Falkowski, L. Ma, W. Lin, *J. Am. Chem. Soc.* 132 (2010) 15390.
- [38] S. Abednatanzi, A. Abbasi, M. Masteri-Farahani, *J. Mol. Catal. A Chem.* 399 (2015) 10.
- [39] D. Jiang, A. Urakawa, M. Yulikov, T. Mallat, G. Jeschke, A. Baiker, *Chem. Eur. J.* 15 (2009) 12255.
- [40] K. Schlichte, T. Kratzke, S. Kaskel, *Microporous and Mesoporous Mater.* 73 (2004) 81.
- [41] H. Liu, Y. Liu, Y. Li, Z. Tang, H. Jiang, *J. Phys. Chem. C.* 114 (2010) 13362.
- [42] D. Jiang, T. Mallat, D.M. Meier, A. Urakawa, A. Baiker, *J. Catal.* 270 (2010) 26.
- [43] M. Annapurna, T. Parsharamulu, P. Vishnuvardhan Reddy, M. Suresh, P.R. Likhar, M. Lakshmi Kantam, *Appl. Organomet. Chem.* 29 (2015) 234.
- [44] J.L. Rowsell, E.C. Spencer, J. Eckert, J.A. Howard, O.M. Yaghi, *Science* 309 (2005) 1350.
- [45] S. Achmann, G. Hagen, J. Kita, I.M. Malkowsky, C. Kiener, R. Moos, *Sens.* 9 (2009) 1574.
- [46] S.M. Humphrey, P.T. Wood, *J. Am. Chem. Soc.* 126 (2004) 13236.
- [47] M. Rubio-Martinez, C. Avci-Camur, A.W. Thornton, I. Imaz, D. Maspoch, M.R. Hill, *Chem. Soc. Rev.* 46 (2017) 3453.
- [48] T. Saeed, A. Naeem, I.U. Din, M.A. Alotaibi, A.I. Alharthi, I.W. Khan, N.H. Khan, T. Malik, *Microchem. J.* 159 (2020) 105579.
- [49] N. Stock, S. Biswas, *Chem. Rev.* 112 (2012) 933.
- [50] Y. Chalati, P. Horcajada, R. Gref, P. Couvreur, C. Serre, *J. Mater. Chem.* 21 (2011) 2220.
- [51] S. Hermes, T. Witte, T. Hikov, D. Zacher, S. Bahnmüller, G. Langstein, K. Huber, R.A. Fischer, *J. Am. Chem. Soc.* 129 (2007) 5324.
- [52] J. Cravillon, S. Muzer, S.-J. Lohmeier, A. Feldhoff, K. Huber, M. Wiebcke, *Chem. Mater.* 21 (2009) 1410.
- [53] F.K. Shieh, S.C. Wang, S.Y. Leo, K.C.W. Wu, *Chem. Eur. J.* 19 (2013) 11139.

- [54] N. Stock, S. Biswas, *Chem. Rev.* 112 (2012) 933.
- [55] V.V.E. Butova, M.A. Soldatov, A.A. Guda, K.A. Lomachenko, C. Lamberti, *Russ. Chem. Rev.* 85 (2016) 280.
- [56] U. Mueller, M. Schubert, F. Teich, H. Puetter, K. Schierle-Arndt, J. Pastre, *J. Mater. Chem.* 16 (2006) 626.
- [57] S. Dai, F. Nouar, S. Zhang, A. Tissot, C. Serre, *Angew. Chem.* 133 (2021) 4328.
- [58] N. Getachew, Y. Chebude, I. Diaz, M. Sanchez-Sanchez, *J. Porous Mater.* 21 (2014) 769.
- [59] J. Jacobsen, A. Ienco, R. D'Amato, F. Costantino, N. Stock, *Dalton Trans.* 49 (2020) 16551.
- [60] Y.K. Hwang, J.S. Chang, S.E. Park, D.S. Kim, Y.U. Kwon, S.H. Jung, J.S. Hwang, M.S. Park, *Angew. Chem. Int. Ed.* 44 (2005) 556.
- [61] S.H. Jung, J.H. Lee, J.W. Yoon, J.S. Hwang, S.E. Park, J.S. Chang, *Microporous and Mesoporous Mater.* 80 (2005) 147.
- [62] G.A. Tompsett, W.C. Conner, K.S. Yngvesson, *ChemPhysChem.* 7 (2006) 296.
- [63] Y.P. Xu, Z.J. Tian, S.J. Wang, Y. Hu, L. Wang, B.C. Wang, Y.C. Ma, L. Hou, J.Y. Yu, Lin, *Angew. Chem. Int. Ed.* 45 (2006) 3965.
- [64] S.H. Jung, J.H. Lee, J.S. Chang, *Bull. Korean Chem. Soc.* 26(2005) 880.
- [65] T. Saeed, A. Naem, I.U. Din, M.A. Alotaibi, A.I. Alharthi, I.W. Khan, N.H. Khan, T. Malik, *Microchem. J.* 159 (2020) 105579.
- [66] A. Stolle, T. Szuppa, S.E. Leonhardt, B. Ondruschka, *Chem. Soc. Rev.* 40 (2011) 2317.
- [67] B. Szczeniak, S. Borysiuk, J. Choma, M. Jaroniec, *Mater. Horiz.* 7 (2020) 1457.
- [68] A.L. Garay, A. Pichon, S.L. James, *Chem Soc Rev.* 36(2007) 846.
- [69] A. Pichon, S.L. James, *Cryst. Eng. Comm.* 10 (2008) 1839.
- [70] T.T. Friščić, D.G. Reid, I. Halasz, R.S. Stein, R.E. Dinnebier, M.J. Duer, *Angew. Chem.* 122 (2010) 724.
- [71] H. Li, M. Eddaoudi, M. O'Keeffe, O.M. Yaghi, *Nature*, 402 (2019) 276.
- [72] J.H. Cavka, S. Jakobsen, U. Olsbye, N. Guillou, C. Lamberti, S. Bordiga, *J. Am. Chem. Soc.* 130 (2008) 13850.
- [73] Z.U. Wang, S.M. Cohen, *Chem. Soc. Rev.* 38 (2009) 1315.
- [74] P.J. Beldon, L. Fábíán, R.S. Stein, A. Thirumurugan, A.K. Cheetham, T. Friščić, *Angew. Chem.* 122 (2010) 9834.
- [75] P.M. Schoenecker, G.A. Belancik, B.E. Grabicka, K.S. Walton, *AIChE J.* 59 (2013) 1255.
- [76] R. Ameloot, F. Vermoortele, W. Vanhove, M.B. Roeffaers, B.F. Sels, D.E. De Vos, *Nat. Chem.* 3 (2011) 382.
- [77] D. Witters, N. Vergauwe, R. Ameloot, S. Vermeir, D. De Vos, R. Puers, B. Sels, J. Lammertyn, *Adv. Mater.* 24 (2012) 1316.
- [78] M. Rubio-Martinez, C. Avci-Camur, A.W. Thornton, I. Imaz, D. MasPOCH, M.R. Hill, *Chem. Soc. Rev.* 46 (2017) 3453.
- [79] A. Carné-Sánchez, I. Imaz, M. Cano-Sarabia, D. MasPOCH, *Nat. Chem.* 5 (2013) 203.
- [80] L. Garzon-Tovar, M. Cano-Sarabia, A. Carné-Sánchez, C. Carbonell, I. Imaz, D. MasPOCH, *React. Chem. Eng.* 1 (2016) 533.
- [81] A. Schoedel, C. Scherb, T. Bein, *Angew. Chem.* 122 (2010) 7383.
- [82] C. Dey, T. Kundu, B.P. Biswal, A. Mallick, R. Banerjee, *Acta. Crystallogr. B. Struct.* 70 (2014) 3.
- [83] A. Gedanken, *Ultrason Sonochem.* 11 (2004) 47.
- [84] N. Stock, S. Biswas, *Chem. Rev.* 112 (2012) 933.
- [85] W.J. Son, J. Kim, J. Kim, W.S. Ahn, *ChemComm.* 47 (2008) 6336.
- [86] Z.Q. Li, L.G. Qiu, W. Wang, T. Xu, Y. Wu, X. Jiang, *Inorg. Chem. Commun.* 11 (2008) 1375.
- [87] Z.Q. Li, L.G. Qiu, T. Xu, Y. Wu, W. Wang, Z.Y. Wu, X. Jiang, *Mater. Lett.* 63 (2009) 78.
- [88] O.K. Farha, A.M. Shultz, A.A. Sarjeant, S.T. Nguyen, J.T. Hupp, *J. Am. Chem. Soc.* 133 (2011) 5652.
- [89] C. Montoro, E. García, S. Calero, M.A. Pérez-Fernández, A.L. López, E. Barea, J.A. Navarro, J. Mater. Chem. 22 (2012) 10155.
- [90] H. Sato, R. Matsuda, K. Sugimoto, M. Takata, S. Kitagawa, *Nat. Mater.* 9 (2010) 661.
- [91] S. Yuan, L. Feng, K. Wang, J. Pang, M. Bosch, C. Lollar, Y. Sun, J. Qin, X. Yang, P. Zhang, Q. Wang, L. Zou, Y. Zhang, L. Zhang, Y. Fang, J. Li, H.C. Zhou, *Adv. Mater.* 30 (2018) 1704303.

- [92] C. Wang, X. Liu, N. Keser Demir, J.P. Chen, K. Li, Chem. Soc. Rev. 45 (2016) 5107.
- [93] M. Ding, X. Cai, H.L. Jiang, Chem. Sci. 10(2019) 10209.
- [94] A.J. Howarth, Y. Liu, P. Li, Z. Li, T.C. Wang, J.T. Hupp, O.K. Farha, Nat. Rev. Mater. 1 (2016) 15018.
- [95] H. Li, W. Shi, K. Zhao, H. Li, Y. Bing, P. Cheng, Inorg. Chem. 51 (2012) 9200.
- [96] J. Canivet, A. Fateeva, Y. Guo, B. Coasne, D. Farrusseng, Chem. Soc. Rev. 43 (2014) 5594.
- [97] X.F. Lu, P.O. Liao, J.W. Wang, J.X. Wu, X.W. Chen, C.T. He, J.P. Zhang, G.R. Li, X.M. Chen, J. Am. Chem. Soc. 138 (2016) 8336.
- [98] K. Wang, X.L. Lv, D. Feng, S. Chen, J. Sun, L. Song, Y. Xie, J.R. Li, H.C. Zhou, J. Am. Chem. Soc. 138 (2016) 914.
- [99] X. Liu, X. Wang, F. Kapteijn, Chem. Rev. 120 (2020) 8303.
- [100] A.J. Rieth, A.M. Wright, M. Dincă, Nat. Rev. Mater. 4 (2019) 708.
- [101] X.L. Lv, K. Wang, B. Wang, J. Su, X. Zou, Y. Xie, J.R. Li, H.C. Zhou, J. Am. Chem. Soc. 139 (2017) 211.
- [102] P.Q. Liao, X.Y. Li, J. Bai, C.T. He, D.D. Zhou, W.X. Zhang, J.P. Zhang, X.M. Chen, Chem. Eur. J. 20 (2014) 11303.
- [103] J.J. Low, A.I. Benin, P. Jakubczak, J.F. Abrahamian, S.A. Faheem, R.R. Willis, J. Am. Chem. Soc. 131 (2009) 15834.
- [104] G. Mouchaham, L. Cooper, N. Guillou, C. Martineau, E. Elkaïm, S. Bourrelly, P.L. Llewellyn, C. Allain, G. Clavier, C. Serre, T. Devic, Angew Chem. 127 (2015) 13495.
- [105] X.L. Lv, K. Wang, B. Wang, J. Su, X. Zou, Y. Xie, J.R. Li, H.C. Zhou, J. Am. Chem. Soc. 139 (2017) 211.
- [106] J. Li, Q.L. Zhu, Q. Xu, Catal. Sci. Technol. 5 (2015) 525.
- [107] G. Lu, S. Li, Z. Guo, O.K. Farha, B.G. Hauser, X. Qi, Y. Wang, X. Wang, S. Han, X. Liu, J.S. DuChene, Nat. Chem. 4 (2012) 310.
- [108] A. Ahmed, M. Forster, R. Clowes, D. Bradshaw, P. Myers, H. Zhang, J. Mater. Chem. A. 1 (2013) 3276.
- [109] I.A. Lázaro, R.S. Forgan, Coord. Chem. Rev. 380 (2019) 230.
- [110] G. Lan, K. Ni, W. Lin, Coord. Chem. Rev. 379 (2019) 65.
- [111] S. Dutta, J. Kim, P.H. Hsieh, Y.S. Hsu, Y.V. Kaneti, F.K. Shieh, Y. Yamauchi, K.C.W. Wu, Small Methods. 3 (2019) 1900213.
- [112] K.B. Wang, Q. Xun, Q. Zhang, Energy Chem. 2 (2020) 100025.
- [113] X. Li, X. Yang, H. Xue, H. Pang, Q. Xu, Energy Chem. 2 (2020) 100027.
- [114] Z. Wu, J. Xie, Z.J. Xu, S. Zhang, Q. Zhang, J. Mater. Chem. A. 7 (2019) 4259.
- [115] K. Sugikawa, S. Nagata, Y. Furukawa, K. Kokado, K. Sada, Chem. Mater. 25 (2013) 2565.
- [116] L.G.K.H.T.JM, R. Ikeda, Y. Kubota, K. Kato, M. Takata, T. Yamamoto, S. Toh, S. Matsumura, H. Iitagawa, Nat. Mater. 13 (2014) 802.
- [117] R. Ameloot, F. Vermoortele, W. Vanhove, M.B. Roeffaers, B.F. Sels, D.E. De Vos, Nat. Chem. 3 (2011) 382.
- [118] K. Khaletskaya, J. Reboul, M. Meilikhov, M. Nakahama, S. Diring, M. Tsujimoto, S. Isoda, F. Kim, K.I. Kamei, R.A. Fischer, S. Kitagawa, 135 (2013) 10998.
- [119] K. Liang, R. Ricco, C.M. Doherty, M.J. Styles, S. Bell, N. Kirby, S. Mudie, D. Haylock, A.J. Hill, C.J. Doonan, P. Falcaro, Nat. Commun. 6 (2015) 7240.
- [120] I. Ghaffar, M. Imran, S. Perveen, T. Kanwal, S. Saifullah, M.F. Bertino, C.J. Ehrhardt, V.K. Yadavalli, M.R. Shah, Mater. Sci. Eng. C 105 (2019) 110111.
- [121] S. Beg, M. Rahman, A. Jain, S. Saini, P. Midoux, C. Pichon, F.J. Ahmad, S. Akhter, Drug Discov. 22 (2017) 625.
- [122] X. Yao, G. Zhu, P. Zhu, J. Ma, W. Chen, Z. Liu, T. Kong, Adv. Funct. Mater. 30 (2020) 1909389.
- [123] P. Horcajada, C. Serre, M. Vallet-Regí, M. Sebban, F. Taulelle, G. Férey, Angew Chem. 118 (2006) 6120.
- [124] X. Zhu, J. Gu, Y. Wang, B. Li, Y. Li, W. Zhao, J. Shi, ChemComm. 50 (2014) 8779.
- [125] P. Horcajada, C. Serre, G. Maurin, N.A. Ramsahye, F. Balas, M. Vallet-Regi, M. Sebban, F. Taulelle, G. Férey, J. Am. Chem. Soc. 130 (2008) 6774.
- [126] J. Zhuang, C.H. Kuo, L.Y. Chou, D.Y. Liu, E. Weerapana, C.K. Tsung, ACS Nano. 8 (2014) 2812.

- [127] H. Zheng, Y. Zhang, L. Liu, W. Wan, P. Guo, A.M. Nyström, X. Zou, *J. Am. Chem. Soc.* 138 (2016) 962.
- [128] L.L. Tan, N. Song, S.X.A. Zhang, H. Li, B. Wang, Y.W. Yang, *J. Mater. Chem. B* 4 (2016) 135.
- [129] N. Motakef-Kazemi, S.A. Shojaosadati, A. Morsali, *Microporous and mesoporous Mater.* 186 (2014) 73.
- [130] L. Zhang, Y. Chen, Z. Li, L. Li, P. Saint-Cricq, C. Li, J. Lin, C. Wang, Z. Su, J.I. Zink, *Angew. Chem. Int. Ed.* 55 (2016) 2118.
- [131] M. Zhang, L. Zhang, Y. Chen, L. Li, Z. Su, C. Wang, *Chem. Sci.* 8 (2017) 8067.
- [132] W.J. Rieter, K.M. Taylor, H. An, W. Lin, W. Lin, *J. Am. Chem. Soc.* 128 (2006) 9024.
- [133] R. Ostermann, J. Cravillon, C. Weidmann, M. Wiebcke, B.M. Smarsly, *ChemComm.* 47 (2011) 442.
- [134] P. Horcajada, T. Chalati, C. Serre, B. Gillet, C. Sebrie, T. Baati, J.F. Eubank, D. Heurtaux, P. Clayette, C. Kreuz, J.S. Chang, *Nat Mater.* 9 (2010) 172.
- [135] H.S. Wang, *Coord. Chem. Rev.* 349 (2017) 139.
- [136] Y. Li, J. Jin, D. Wang, J. Lv, K. Hou, Y. Liu, C. Chen, Z. Tang, *Nano Research*, 11 (2018) 3294.
- [137] C. He, K. Lu, W. Lin, *J. Am. Chem. Soc.* 136 (2014) 12253.
- [138] S. Zhang, X. Pei, H. Gao, S. Chen, J. Wang, *Chin Chem Lett.* 31 (2020) 1060.
- [139] W. Liu, Y.M. Wang, Y.H. Li, S.J. Cai, X.B. Yin, X.W. He, Y.K. Zhang, *Small* 13 (2017) 1603459.
- [140] S. Chernousova, M. Epple, *Angew. Chem. Int. Ed.* 52 (2013) 1636.
- [141] M. Chen, Z. Long, R. Dong, L. Wang, J. Zhang, S. Li, X. Zhao, X. Hou, H. Shao, X. Jiang, *Small* 16 (2020) 1906240.
- [142] P. Li, J. Li, X. Feng, J. Li, Y. Hao, J. Zhang, H. Wang, A. Yin, J. Zhou, X. Ma, B. Wang, *Nat. Commun.* 10 (2019) 2177.
- [143] P. Huang, J. Lin, X. Wang, Z. Wang, C. Zhang, M. He, K. Wang, F. Chen, Z. Li, G. Shen, D. Cui, *Adv. Mater.* 24 (2012) 5104.
- [144] J.S. Kahn, L. Freage, N. Enkin, M.A.A. Garcia, I. Willner, *Adv Mater.* 29 (2017) 1602782.
- [145] L. Zhang, Q. Cheng, C. Li, X. Zeng, X.Z. Zhang, *Biomaterials* 248 (2020) 120029.
- [146] B. Claes, T. Boudewijns, L. Muchez, G. Hooyberghs, E.V. Van der Eycken, J. Vanderleyden, H.P. Steenackers, D.E. De Vos, *ACS Appl. Mater. Interfaces.* 9 (2017) 4440.
- [147] S. Lin, X. Liu, L. Tan, Z. Cui, X. Yang, K.W. Yeung, H. Pan, S. Wu, *ACS Appl. Mater. Interfaces.* 9 (2017) 19248.
- [148] J. Chen, X. Zhang, C. Huang, H. Cai, S. Hu, Q. Wan, X. Pei, J. Wang, *J. Biomed. Mater. Res. A.* 105 (2017) 834.
- [149] X.P. Wang, J. Hou, F.S. Chen, X.M. Meng, *Sep. Purif. Technol.* 236 (2020) 116239.
- [150] X. Ren, C. Yang, L. Zhang, S. Li, S. Shi, R. Wang, X. Zhang, T. Yue, J. Sun, J. Wang, *Nanoscale* 11 (2019) 11830.
- [151] I. Nath, J. Chakraborty, F. Verpoort, *Chem. Soc. Rev.* 45 (2016) 4127.
- [152] C.D. Wu, M. Zhao, *Advanced Materials* 29 (2017) 1605446.
- [153] J.W. Zhang, H.T. Zhang, Z.Y. Du, X. Wang, S.H. Yu, H.L. Jiang, *ChemComm.* 50 (2014) 1092.
- [154] M. Zhao, C.D. Wu, *Chem. Cat. Chem.* 9 (2017) 1192.
- [155] C.D. Wu, M. Zhao, *Adv. Mater.* 29 (2017) 1605446.
- [156] Y.K. Park, S.B. Choi, H. Kim, K. Kim, B.H. Won, K. Choi, J.S. Choi, W.S. Ahn, N. Won, S. Kim, D.H. Jung, *Angew. Chem. Int. Ed.* 46 (2007) 8230.
- [157] X. Wu, J. Ge, C. Yang, M. Hou, Z. Liu, *Chem. Comm.* 51 (2015) 13408.
- [158] H. Anwer, A. Mahmood, J. Lee, K.H. Kim, J.W. Park, A.C. Yip, *Nano Res.* 12 (2019) 955.
- [159] C.V. Reddy, K.R. Reddy, V.V. N. Harish, J. Shim, M.V. Shankar, N.P. Shetti, T.M. Aminabhavi, *Int. J. Hydrog. Energy.* 45 (2020) 7656.
- [160] A. Rafiq, M. Ikram, S. Ali, F. Niaz, M. Khan, Q. Khan, M. Maqbool, *J. Ind. Eng. Chem.* 97 (2021) 111.
- [161] P. Liang, C. Zhang, H. Sun, S. Liu, M. Tadé, S. Wang, *RSC Adv.* 6 (2016) 95903.
- [162] R. Kamandi, N.M. Mahmoodi, M. Kazemini, *Mater. Chem. Phys.* 269 (2021) 124726.
- [163] Y.L. Wang, S. Zhang, Y.F. Zhao, J. Bedia, J.J. Rodriguez, C. Belver, *J. Environ. Chem. Eng.* 9 (2021) 106087.

- [164] W. Huang, N. Liu, X. Zhang, M. Wu, L. Tang, *Appl. Surf. Sci.* 425 (2017) 107.
- [165] B. Hu, J.Y. Yuan, J.Y. Tian, M. Wang, X. Wang, L. He, Z. Zhang, Z.W. Wang, C.S. Liu, *Colloid Interface Sci.* 531 (2018) 148.
- [166] J. Li, X. Xu, X. Liu, W. Qin, M. Wang, L. Pan, *J. Alloys Compd.* 690 (2017) 640.
- [167] S.J. Yang, J.H. Im, T. Kim, K. Lee, C.R. Park, *J. Hazard. Mater.* 186 (2011) 376.
- [168] Y. Lin, H. Wan, F. Chen, X. Liu, R. Ma, T. Sasaki, *Dalton Trans.* 47 (2018) 7694.
- [169] C. Zhang, D. Guo, T. Shen, X. Hou, M. Zhu, S. Liu, Q. Hu, *Colloids Surf. A: Physico Chem. Eng. Asp.* 589 (2020) 124484.
- [170] T. Tang, X. Jin, X. Tao, L. Huang, S. Shang, *J. Alloys Compd.* 895 (2022) 162452.
- [171] J.M. Yassin, A.M. Taddesse, M. Sánchez-Sánchez, *Appl. Surf. Sci.* 578 (2022) 151996.
- [172] Y. Zhang, G. Li, GQ. Guo, *Microporous and Mesoporous Mater.* 324 (2021) 111291.
- [173] X. Xuan, M. Qian, L. Pan, T. Lu, L. Han, H. Yu, L. Wan, Y. Niu, S. Gong, *J. Mater. Chem. B.* 8 (2020) 9094.
- [174] H. Jia, N. Shang, Y. Feng, H. Ye, J. Zhao, H. Wang, C. Wang, Y. Zhang, *J. Colloid Interface Sci.* 58 (2021) 310.
- [175] B. Li, T. Suo, S. Xie, A. Xia, Y.J. Ma, H. Huang, X. Zhang, Q. Hu, *TrAC - Trends Anal. Chem.* 135 (2021) 116163.
- [176] C.S. Liu, J. Li, H. Pang, *Coord. Chem. Rev.* 410 (2020) 213222.
- [177] A. Domenech, H. García, M.T. Doménech-Carbó, F. Llabrés-i-Xamena, *J. Phys. Chem. C.* 111 (2007) 13701.
- [178] B. Yuan, R. Zhang, X. Jiao, J. Li, H. Shi, D. Zhang, *Electrochem. Commun.* 40 (2014) 92.
- [179] T. Yang, H. Yang, S.J. Zhen, C.Z. Huang, *ACS Appl. Mater. Interfaces.* 7 (2015) 1586.
- [180] M. Saraf, R. Rajak, S.M. Mobin, *J. Mater. Chem. A.* 4 (2016) 16432.
- [181] M. Deng, S. Lin, X. Bo, L. Guo, *Talanta* 174 (2017) 527.
- [182] Z. Peng, Z.Jiang, X. Huang, Y. Li, *RSC Adv.* 6 (2016) 13742.
- [183] G. Gumilar, Y.V. Kaneti, J. Henzie, S. Chatterjee, J. Na, B. Yulianto, N. Nugraha, A. Patah, A. Bhaumik, Y. Yamauchi, *Chem. Sci.* 11 (2020) 3644.
- [184] N. Yang, K. Guo, Y. Zhang, C. Xu, *J. Mater. Chem. B.* 8 (2020) 2856.
- [185] L. Shi, Y. Li, X. Cai, H. Zhao, M. Lan, *J. Electroanal. Chem.* 799 (2017) 512.
- [186] Y. Sun, Y. Li, N. Wang, Q.Q. Xu, L. Xu, M. Lin, *Electroanalysis.* 30 (2018) 474.
- [187] D. Arif, Z. Hussain, M. Sohail, M.A. Liaqat, M.A. Khan, T. Noor, *Front. Chem.* 8 (2020) 573510.
- [188] W. Meng, Y. Wen, L. Dai, Z. He, L. Wang, *Sens. Actuators B: Chem.* 260 (2018) 852.
- [189] A.D. Daud, H.N. Lim, I. Ibrahim, N.A. Endot, N.S.K. Gowthaman, Z.T. Jiang, K.E. Cordova, *J. Electroanal. Chem.* 92 (2022) 116676.
- [190] W. Zhang, G. Jia, Z. Li, C. Yuan, Y. Bai, D. Fu, *Adv. Mater. Interfaces.* 4 (2017) 1601241.
- [191] Y. Wang, L. Wang, W. Huang, T. Zhang, X. Hu, J.A. Perman, S. Ma, *J. Mater. Chem. A.* 5 (2017) 8385.
- [192] S.K. Sahoo, G.D. Kim, H.J. Choi, *J. Photochem. Photobiol. C: Photochem.* 27 (2016) 30.
- [193] V. Chandrasekhar, P. Bag, M.D. Pandey, *Tetrahedron.* 65 (2009) 9876.
- [194] A. Hussen, *AJST.* 3 (2021) 69.
- [195] Z. Liu, W. He, Z. Guo, *Chem. Soc. Rev.* 42 (2013) 1568.
- [196] W.P. Lustig, S. Mukherjee, N.D. Rudd, A.V. Desai, J. Li, S.K. Ghosh, *Chem. Soc. Rev.* 46 (2017) 3242.
- [197] X. Zhang, Q. Zhang, D. Yue, J. Zhang, J. Wang, B. Li, Y. Yang, Y. Cui, G. Qian, *Small.* 14 (2018) 1801563.
- [198] Y. Zhang, S. Yuan, G. Day, X. Wang, X. Yang, H.C. Zhou, *Coord. Chem. Rev.* 354 (2018) 28.
- [199] J. Chen, H. Chen, T. Wang, J. Li, J. Wang, X. Lu, *Anal. Chem.* 91 (2019) 4331.
- [200] T. Zhong, D. Li, C. Li, Z. Zhang, G. Wang, *Anal. Methods* 14 (2022) 2714.
- [201] H. Xu, J. Gao, X. Qian, J. Wang, H. He, Y. Cui, Y. Yang, Z. Wang, G. Qian, *J. Mater. Chem. A* 4 (2016) 10900.
- [202] Y. Zhao, X. Zhai, L. Shao, L. Li, Y. Liu, X. Zhang, J. Liu, F. Meng, Y. Fu, *J. Mater. Chem. C* 9 (2021) 15840.

- [203] Z. Zhang, Z. Wei, F. Meng, J. Su, D. Chen, Z. Guo, H. Xing, *Chem. Eur. J.* 26 (2020) 1661.
- [204] R. Puglisi, A.L. Pellegrino, R. Fiorenza, S. Scirè, G. Malandrino, *Sensors* 21 (2021) 1679.
- [205] H. Li, D. Li, B. Qin, W. Li, H. Zheng, X. Zhang, J. Zhang, *Dyes Pigm.* 178 (2020) 108359.
- [206] J. Liu, X. Wang, Y. Zhao, Y. Xu, Y. Pan, S. Feng, J. Liu, X. Huang, H. Wang, *Anal. Chem.* 94 (2022) 10091.
- [207] C. Fan, X. Lv, M. Tian, Q. Yu, Y. Mao, W. Qiu, H. Wang, G. Liu, *Mikrochim. Acta* 187 (2020) 1.
- [208] Y.A. Li, S. Yang, Q.Y. Li, J.P. Ma, S. Zhang, Y.B. Dong, *Inorg. Chem.* 56 (2017) 13241.
- [209] T. Lu, L. Zhang, M. Sun, D. Deng, Y. Su, Y. Lv, *Anal. Chem.* 88 (2016) 3413.
- [210] Z. Zhou, X. Li, Y. Tang, C.C. Zhang, H. Fu, N. Wu, L. Ma, J. Gao, Q. Wang, *J. Chem. Eng.* 351 (2018) 364.
- [211] X. Gao, G. Sun, X. Wang, X. Lin, S. Wang, Y. Liu, *Sens. Actuators B: Chem.* 331 (2021) 129448.
- [212] Z. Sun, J. Li, X. Wang, Z. Zhao, R. Lv, Q. Zhang, F. Wang, Y. Zhao, *J. Lumin.* 241 (2022) 118480.
- [213] A. Afzalnia, M. Mirzaee, *ACS Appl. Mater. Interfaces.* 12 (2020) 16076.
- [214] X. Huang, Z. He, D. Guo, Y. Liu, J. Song, B.C. Yung, L. Lin, G. Yu, J.J. Zhu, Y. Xiong, X. Chen, *Theranostics.* 8 (2018) 3461.
- [215] A.S. Basaleh, S.M. Sheta, *Anal. Bioanal. Chem.* 412 (2020) 3153.
- [216] S. Venkateswarlu, A.S. Reddy, A. Panda, D. Sarkar, Y. Son, M. Yoon, *ACS Appl. Nano Mater.* 3 (2020) 3684.
- [217] X.Y. Xu, B. Yan, *Adv. Funct. Mater.* 27 (2017) 1700247.
- [218] A. Karmakar, N. Kumar, P. Samanta, A.V. Desai, S.K. Ghosh, *Chem. Eur. J.* 22 (2016) 864.
- [219] K. Vikrant, D.C. Tsang, N. Raza, B.S. Giri, D. Kukkar, K.H. Kim, *ACS Appl. Mater. Interfaces.* 10 (2018) 8797.
- [220] H. Tian, H. Fan, M. Li, L. Ma, *ACS Sensors* 1 (2016) 243.
- [221] C.P. Li, W.W. Long, Z. Lei, L. Guo, M.J. Xie, J. Lü, X.D. Zhu, *ChemComm.* 56 (2020) 12403.
- [222] X. Zhang, Q. Ma, X. Liu, H. Niu, L. Luo, R. Li, X. Feng, *Food Chem.* 382 (2022) 132379.
- [223] X. Zhang, Q. Hu, T. Xia, J. Zhang, Y. Yang, Y. Cui, B. Chen, G. Qian, *ACS Appl. Mater. Interfaces.* 8 (2016) 32259.
- [224] J. Guo, L. Yang, Z. Gao, C. Zhao, Y. Mei, Y.Y. Song, *ACS Catal.* 10 (2020) 5949.
- [225] L.M. Kustov, V.I. Isaeva, J. Přeck, K.K. Bisht, *Mendeleev Commun.* 29 (2019) 361.
- [226] S. Kitagawa, *Chem. Soc. Rev.* 43 (2014) 5415.
- [227] J.R. Long, O.M. Yaghi, *Chem Soc Rev.* 38 (2009) 1213.
- [228] F. Yu, X. Bai, M. Liang, J. Ma, *J. Chem. Eng.* 405 (2021) 126960.
- [229] S.A. Younis, N. Bhardwaj, S.K. Bhardwaj, K.H. Kim, A. Deep, *Coord. Chem. Rev.* 429 (2021) 213620.
- [230] S. Pan, X. Chen, X. Li, M. Jin, *J. Sep. Sci.* 42 (2019) 1045.
- [231] A. Ghanem, P. Bados, L. Kerhoas, J. Dubroca, J. Einhorn, *Anal. Chem.* 79 (2007) 3794.
- [232] L.L. Ma, G.P. Yang, G.P. Li, P.F. Zhang, J. Jin, Y. Wang, J.M. Wang, Y.Y. Wang, *Inorg. Chem. Front.* 8 (2021) 329.
- [233] T. Chowdhury, L. Zhang, J. Zhang, S. Aggarwal, *Nanomaterials.* 8 (2018) 1062.
- [234] L. Ullah, G. Zhao, N. Hedin, X. Ding, S. Zhang, X. Yao, Y. Nie, Y. Zhang, *J. Chem. Eng.* 362 (2019) 30.
- [235] A. Hamed, M.B. Zarandi, M.R. Nateghi, *J. Environ. Chem. Eng.* 7 (2019) 102882.
- [236] A. Jarrah, S. Farhadi, *Acta Chim. Slov.* 66 (2019) 85.
- [237] A.S. Bhowan, B.C. Freeman, *Environ. Sci. Technol.* 45 (2011) 8624.
- [238] M.E. Boot-Handford, J.C. Abanades, E.J. Anthony, M.J. Blunt, S. Brandani, N. Mac Dowell, J.R. Fernández, M.C. Ferrari, R. Gross, J.P. Hallett, R.S. Haszeldine, *Energy Environ. Sci.* 7 (2014) 130.
- [239] M.A. Sabri, S. Al Jitan, D. Bahamon, L.F. Vega, G. Palmisano, *Sci. Total Environ.* 790 (2021) 148081.
- [240] R. Aniruddha, I. Sreedhar, B.M. Reddy, *J. CO₂ Util.* 42 (2020) 101297.
- [241] T. Ghanbari, F. Abnisa, W.M.A.W. Daud, *Sci. Total Environ.* 707 (2020) 135090.
- [242] Y. Li, J. Miao, X. Sun, J. Xiao, Y. Li, H. Wang, Q. Xia, Z. Li, *J. Chem. Eng.* 298 (2016) 191.

- [243] J. Pokhrel, N. Bhorla, C. Wu, K. S, K, Reddy, H. Margetis, S. Anastasiou, G. George, V. Mittal, G. Romanos, D. Karonis, G.N. Karanikolos, *J. Solid State Chem.* 266 (2018) 233.
- [244] S. Shang, Z. Tao, C. Yang, A. Hanif, L. Li, D.C. Tsang, Q. Gu, J. Shang, *J. Chem. Eng.* 393 (2020) 124666.
- [245] S. Ullah, A.M. Shariff, M.A. Bustam, A.E.I. Elkhalfah, G. Gonfa, F.A.A. Kareem, *J. Chin. Chem. Soc.* 63 (2016) 1022.
- [246] A. Kronast, S. Eckstein, P.T. Altenbuchner, K. Hindelang, S.I. Vagin, B. Rieger, *Chem. Eur. J.* 22 (2016) 12800.
- [247] J. An, S.J. Geib, N.L. Rosi, *J. Am. Chem. Soc.* 132 (2010) 38.
- [248] S. Couck, J.F. Denayer, G.V. Baron, T. Rémy, J. Gascon, F. Kapteijn, *J. Am. Chem. Soc.* 131 (2009) 6326.
- [249] S.R. Caskey, A.G. Wong-Foy, A.J. Matzger, *J. Am. Chem. Soc.* 130 (2008) 10870.
- [250] S. Surblé, F. Millange, C. Serre, T. Düren, M. Latroche, S. Bourrelly, P.L. Llewellyn, G. Férey, *J. Am. Chem. Soc.* 128 (2006) 14889.
- [251] L.A. Darunte, A.D. Oetomo, K.S. Walton, D.S. Sholl, C.W. Jones, *ACS Sustain. Chem. Eng.* 4 (2016) 5761.
- [252] J.B. Goodenough, *Energy Environ. Sci.* 7 (2014) 14.
- [253] R. Vinodh, Y. Sasikumar, H.J. Kim, R. Atchudan, M. Yi, *J Ind Eng Chem.* 104 (2021) 155.
- [254] I. Kim, R. Vinodh, C.V.M. Gopi, H.J. Kim, R.S. Babu, C. Deviprasath, M. Devendiran, S. Kim, *J. Energy Storage.* 43 (2021) 103287.
- [255] R. Atchudan, K. Samikannu, S. Perumal, T.N.J.I. Edison, R. Vinodh, Y.R. Lee, *Mater. Lett.* 30 (2022) 131445.
- [256] R. Atchudan, T.N.J.I. Edison, S. Perumal, R. Vinodh, R.S. Babu, A.K. Sundramoorthy, A.A. Renita, Y.R. Lee, *Chemosphere.* 289 (2022) 133225.
- [257] R. Kötz, M.J.E.A. Carlen, *Electrochim. Acta.* 45 (2000) 2483.
- [258] A.R. Selvaraj, A. Muthusamy, H.J. Kim, K. Senthil, K. Prabakar, *Carbon.* 174 (2021) 463.
- [259] R. Ramya, R. Sivasubramanian, M.V. Sangaranarayanan, *Electrochim. Acta.* 101 (2013) 109.
- [260] G.A. Snook, P. Kao, A.S. Best, *J. Power Sources.* 196 (2011) 1.
- [261] D.P. Dubal, R. Holze, *J. Power Sources.* 238 (2013) 274.
- [262] F. Yang, H. Sadam, Y. Zhang, J. Xia, X. Yang, J. Long, S. Li, L. Shao, *Chem. Eng. Sci.* 225 (2020) 115845.
- [263] P. Srimuk, S. Luanwuthi, A. Krittayavathananon, M. Sawangphruk, *Electrochim. Acta* 157 (2015) 69.
- [264] Y. Zhou, Z. Mao, W. Wang, Z. Yang, X. Liu, *ACS Appl. Mater. Interfaces.* 8 (2016) 28904.
- [265] A. Hosseinian, A. Amjad, R. Hosseinzadeh-Khanmiri, E. Ghorbani-Kalhor, M. Babazadeh, E. Vessally, *J. Mater. Sci. Mater.* 28 (2017) 18040.
- [266] X. Bai, Q. Liu, Z. Lu, J. Liu, R. Chen, R. Li, D. Song, X. Jing, P. Liu, J. Wang, *ACS Sustain. Chem. Eng.* 5 (2017) 9923.
- [267] S. Chen, M. Xue, Y. Li, Y. Pan, L. Zhu, S. Qiu, *J. Mater. Chem. A* 3 (2015) 20145.
- [268] Y. Dong, Y. Wang, Y. Xu, C. Chen, Y. Wang, L. Jiao, H. Yuan, *Electrochim. Acta* 225 (2017) 39.
- [269] X. Cao, B. Zheng, W. Shi, J. Yang, Z. Fan, Z. Luo, X. Rui, B. Chen, Q. Yan, H. Zhang, *Adv. Mater.* 27 (2015) 4695.
- [270] P.C. Banerjee, D.E. Lobo, R. Middag, W.K. Ng, M.E. Shaibani, M. Majumder, *ACS Appl. Mater. Interfaces.* 7 (2015) 3655.
- [271] X.W. Hu, S. Liu, B.T. Qu, X.Z. You, *ACS Appl. Mater. Interfaces.* 7 (2015) 9972.
- [272] C. Guan, X. Liu, W. Ren, X. Li, C. Cheng, J. Wang, *Adv. Energy Mater.* 7 (2017) 1602391.